

Search for a doubly-charged Higgs through vector boson fusion in the Georgi-Machacek model

for the 2017 CAP Congress

by Jérôme Claude

Supervisors: Jean-François Arguin, Georges Azuelos



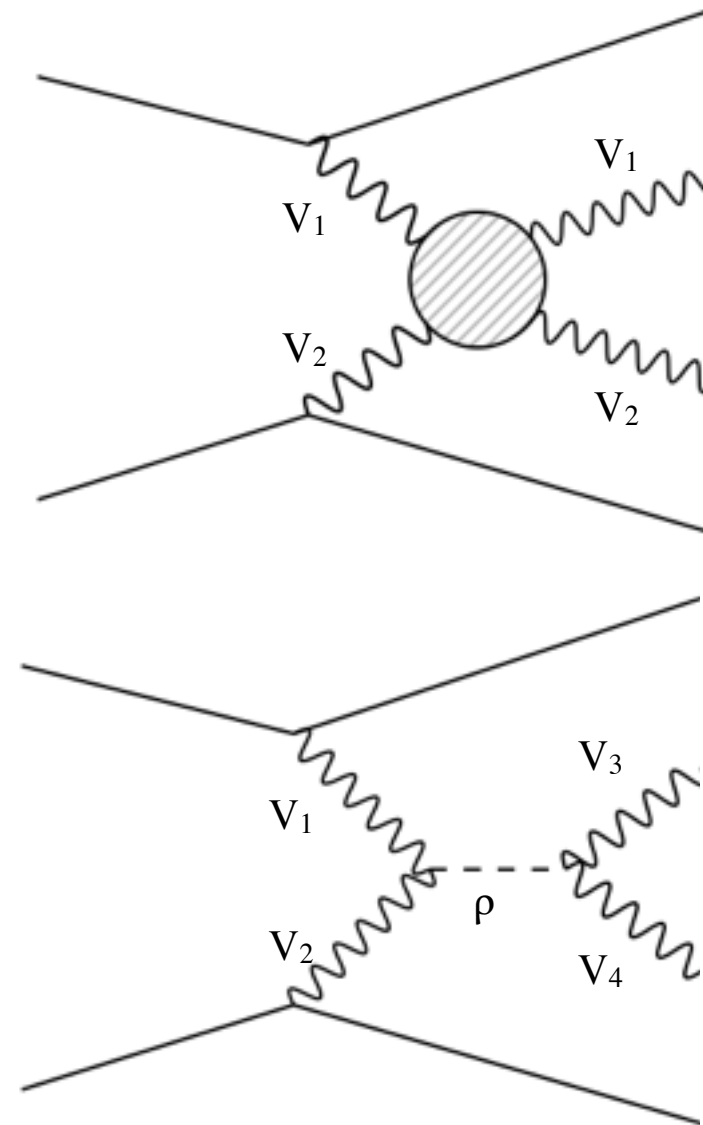
Motivation

Vector boson scattering (VBS) and fusion (VBF) processes feature characteristic hard forward jets.

These processes are unitarized by the SM Higgs boson. If the scalar detected at the LHC in 2012 is not the SM Higgs, then there is room for new resonances.

Same-sign signatures are rare in the SM.

There are models which extend the Higgs sector with triplets or higher multiplets, giving rise to a doubly-charged Higgs boson (DCH).

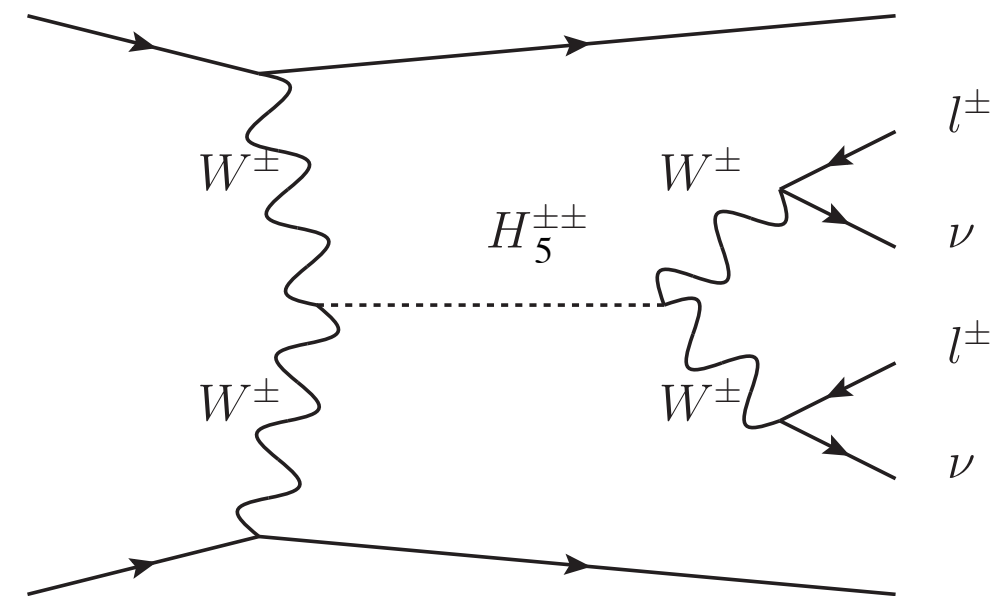


Phenomenology

We consider the Georgi–Machacek model.

H. Georgi and M. Machacek, Nucl. Phys. B 262, 463 (1985).

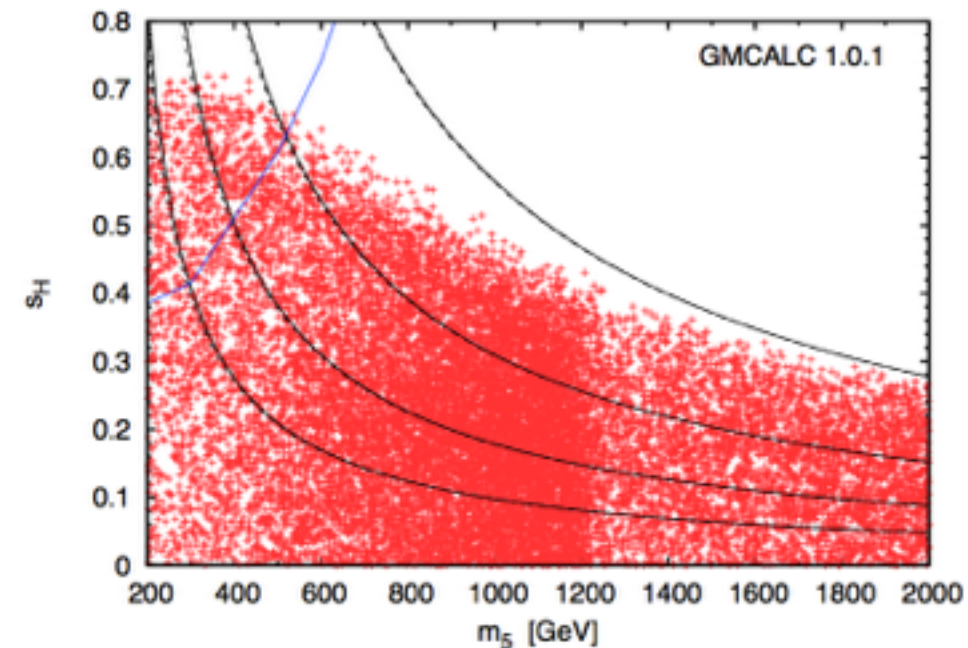
- Adds two triplets to the scalar sector.
- Conserves custodial SU(2) symmetry, and is the least constrained of all Higgs triplet models.
- Results in ten Higgs bosons: two singlets, a triplet and a quintuplet.
- The quintuplet is fermiophobic, and its $H^{\pm\pm}$ can be produced through VBF and has a same-sign leptons final state.



Generation of the signal samples

GM model has 8 parameters, but only three are relevant for vector boson couplings: m_h , m_{H5} , $\sin\theta_H$.

Generation at LO using MadGraph with $H^{\pm\pm}$ mass from 200 GeV to 900 GeV in 100 GeV steps, with $\sin\theta_H=0.5$.



H_5 benchmark @
InspireHEP:[1400940](https://arxiv.org/abs/1400940)

Cross-section scaling: $\sigma/\sin^2\theta_H$ is a constant.

Parameter card generated by GMCALC software (developed by K. Hartling, K. Kumar & H. Logan).

GMCALC @ arXiv:[1412.7387](https://arxiv.org/abs/1412.7387)

Tag jets in VBS events

VBS analyses use various methods to choose tagging jets (the forward, signature jets of VBS). These include:

- Two jets with highest p_T
- Two jets with greatest E
- Jets with greatest $\Delta\eta$ (among three with highest p_T)

In this analysis, we use any pair of jets among the three with highest p_T as long as they pass the m_{jj} cut the Δy_{jj} cut and the opposite hemisphere requirement.

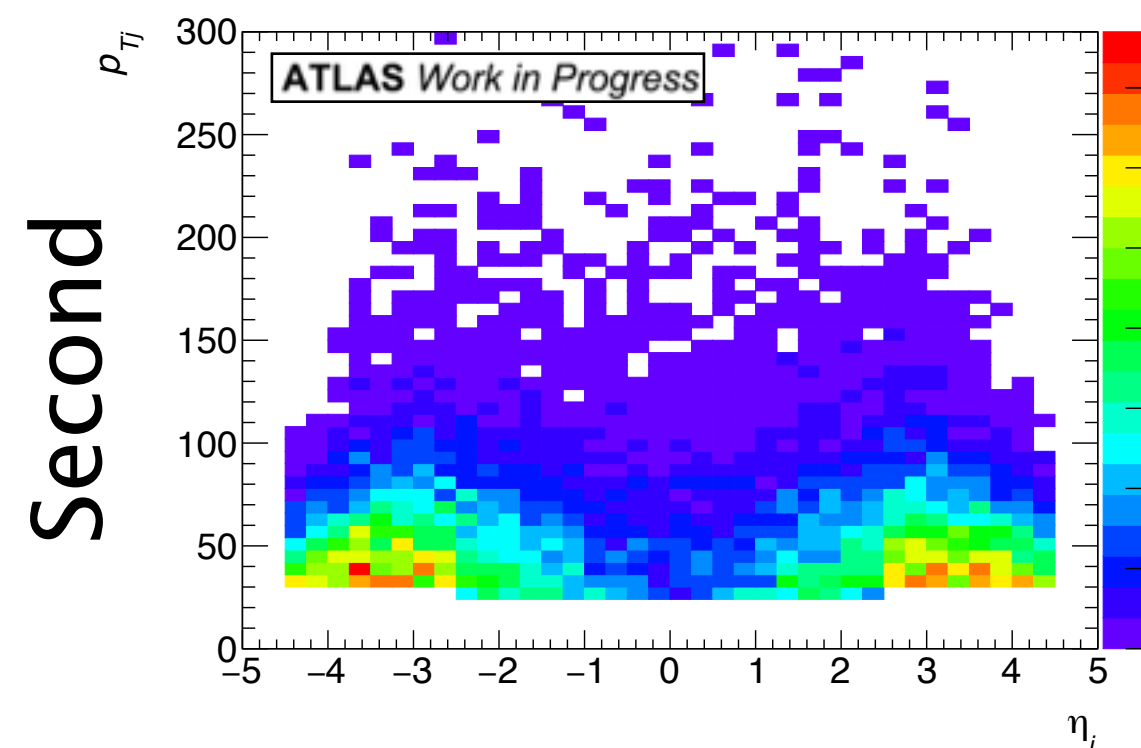
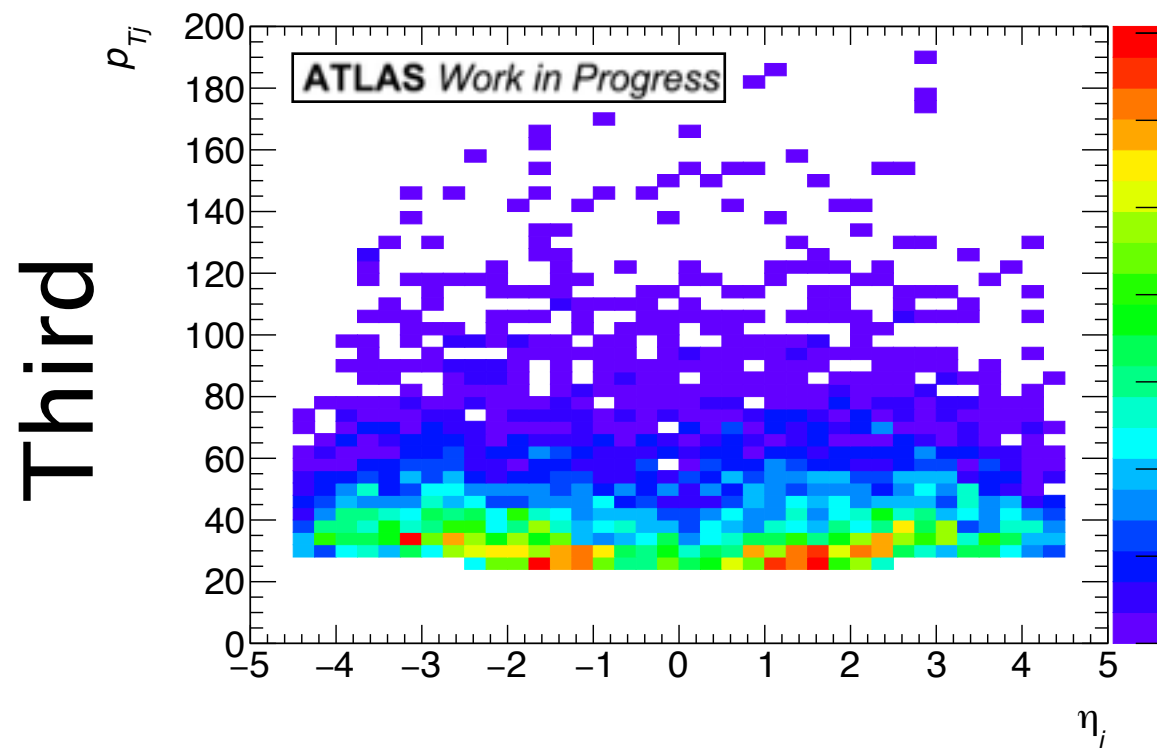
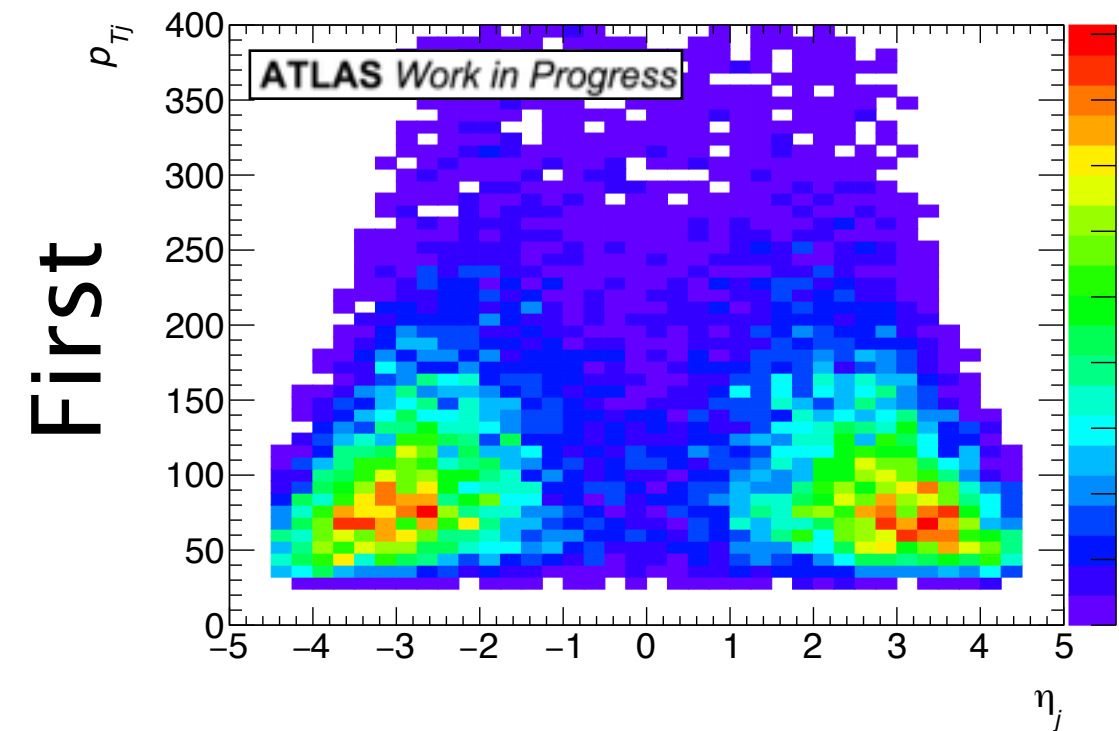
(y and η are measures of the angle to the beam axis).

Tag jets in VBS events

The order of preference is:

1. First and second
2. First and third
3. Second and third

Even the third jet sometimes exhibits VBS-like characteristics.



Charge-flip

There are very few processes in the SM that produce same-sign leptons.

Most background comes from charge-flip effects (e.g. in Z/γ^* decays or W^+W^- decays).



Bad track reconstruction



Bremsstrahlung

Cuts are implemented to remove these processes

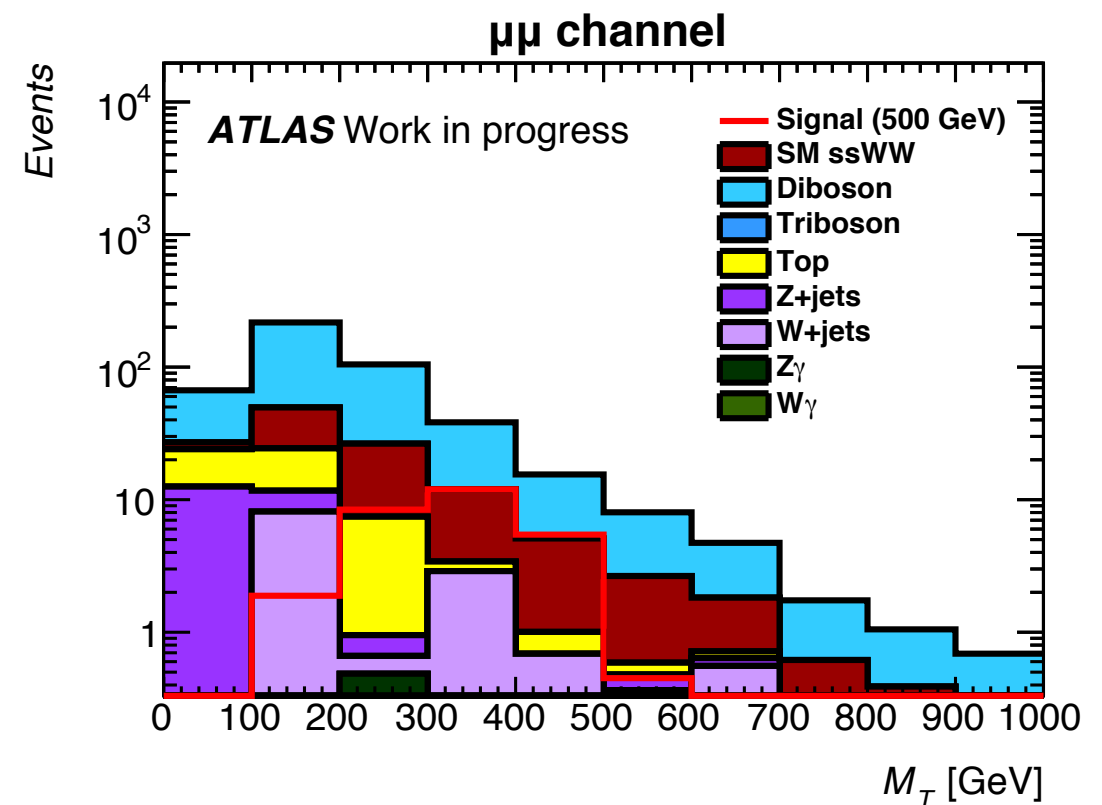
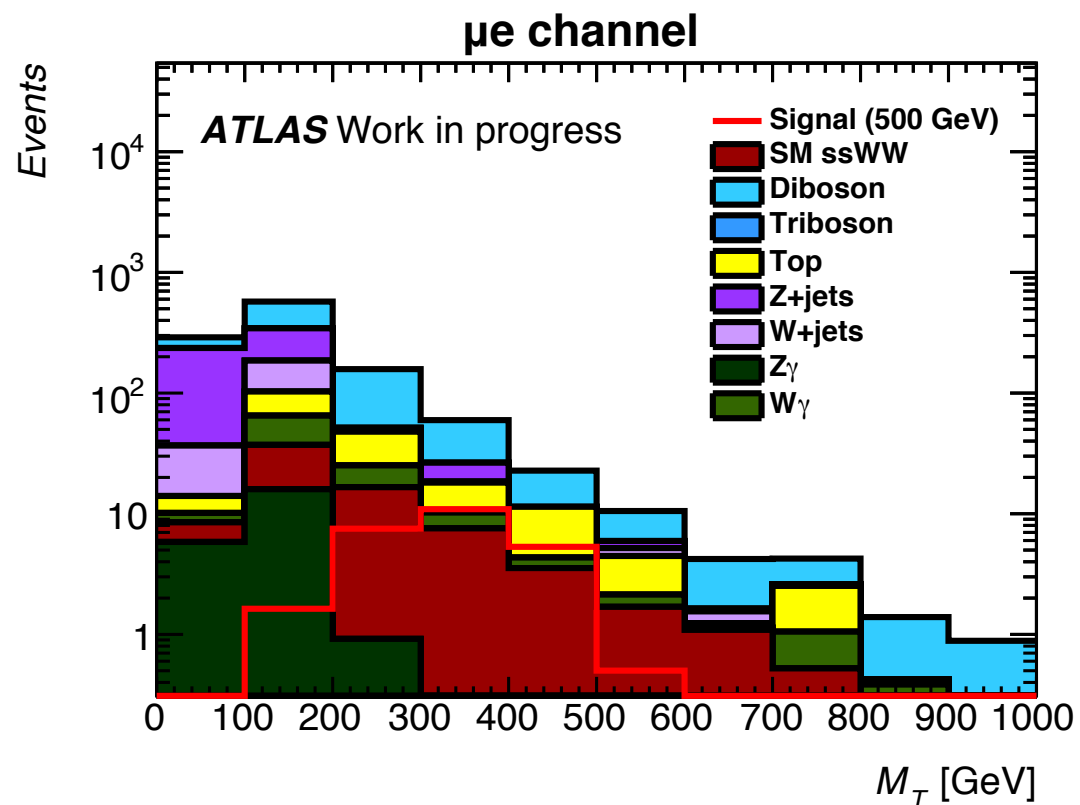
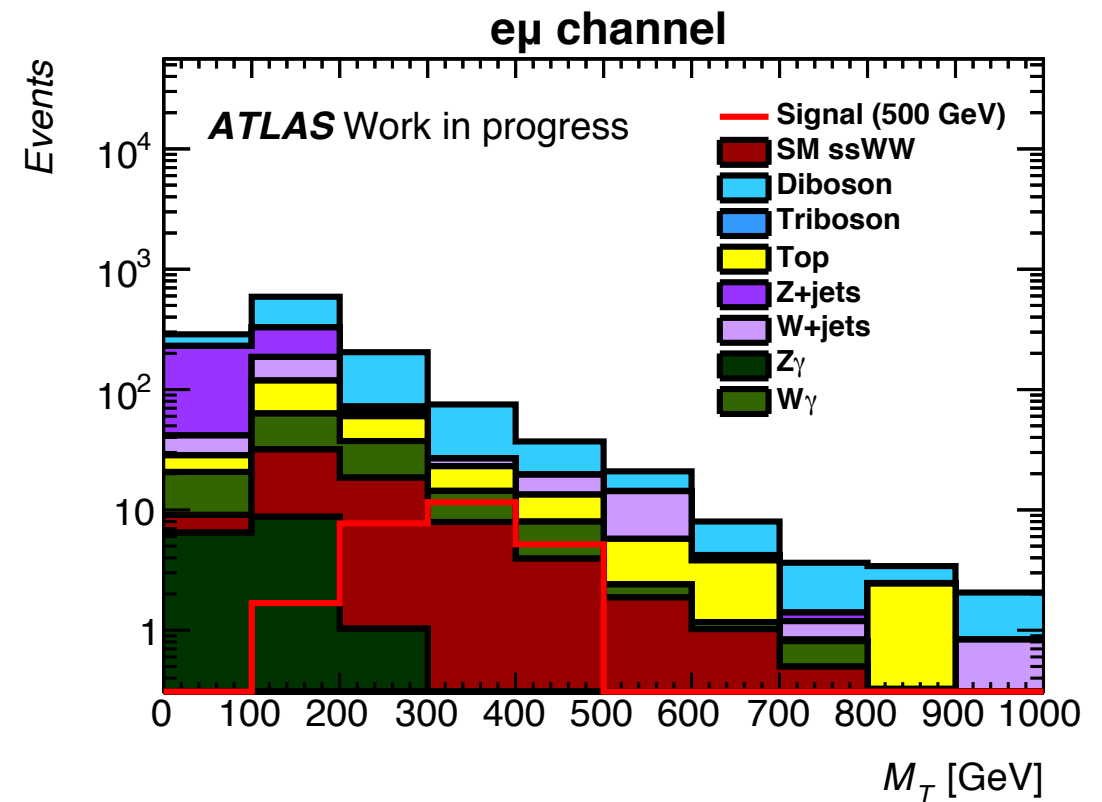
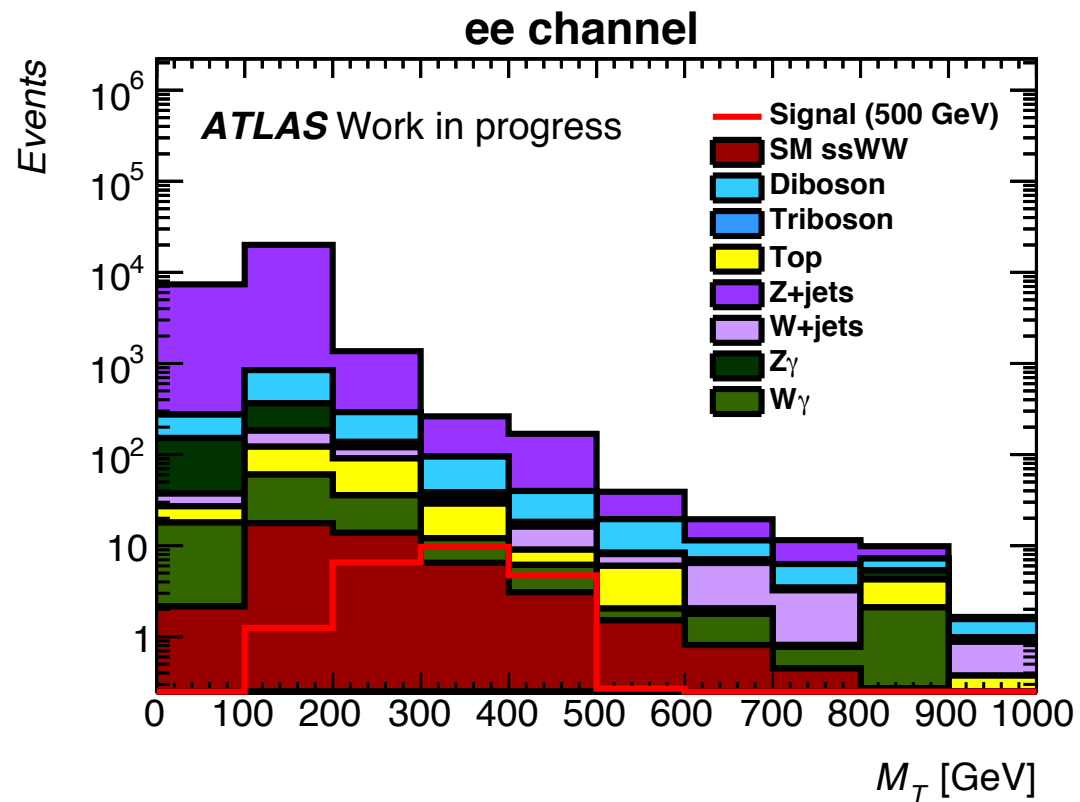
Pre-selection cuts

The following cuts are applied prior to the cut optimization process:

- Exactly two same-sign leptons with $p_T > 20$ GeV
- Dilepton mass not within 10 GeV of Z mass (ee only)
- $|\eta_e| < 1.37$ (to reduce charge-flip)
- At least two jets with $p_T > 30$ GeV and $|\eta| < 4.5$
- b-jet veto at 85% efficiency

These cuts are applied to all figures in this talk.

Background composition (36 fb⁻¹)



Square cut optimization

To isolate signal from background, we apply cuts on the following quantities: m_{jj} , Δy_{jj} , m_{ll} , Δy_{ll} , $E_{T\text{miss}}$.

As a measure of cut set performance, we use the Asimov approximation for median significance:

$$\sigma = \sqrt{\sum_i 2(S_i + B_i) \log\left(1 + \frac{S_i}{B_i}\right) - S_i}$$

This quantity is calculated per bin of the reconstructed mass histogram (m_{1T}). The histogram has 25 bins.

Optimization process outputs the significance for each possible cut configuration in the 5D space.

Square cut optimization results

The optimal cuts follow the following pattern:

- High m_{jj} cut, high jet separation (VBS jets).
- m_{ll} increasing with resonance mass, low lepton separation (leptons originate from resonance).
- $E_{T\text{miss}}$ cut only used for ee channel, decreases with resonance mass (back-to-back neutrinos). Replaces lepton separation requirement at low masses.

Low significance for ee channel (4 to 3.5). For other channels, higher significance at lower resonance masses (7.5 to 3).

Multivariate analysis

We are also considering cut optimization through a multivariate analysis (MVA) using the Root TMVA tool.

This is a type of machine learning: software is fed information with "answer key" and devises a way to answer the question for similar information.

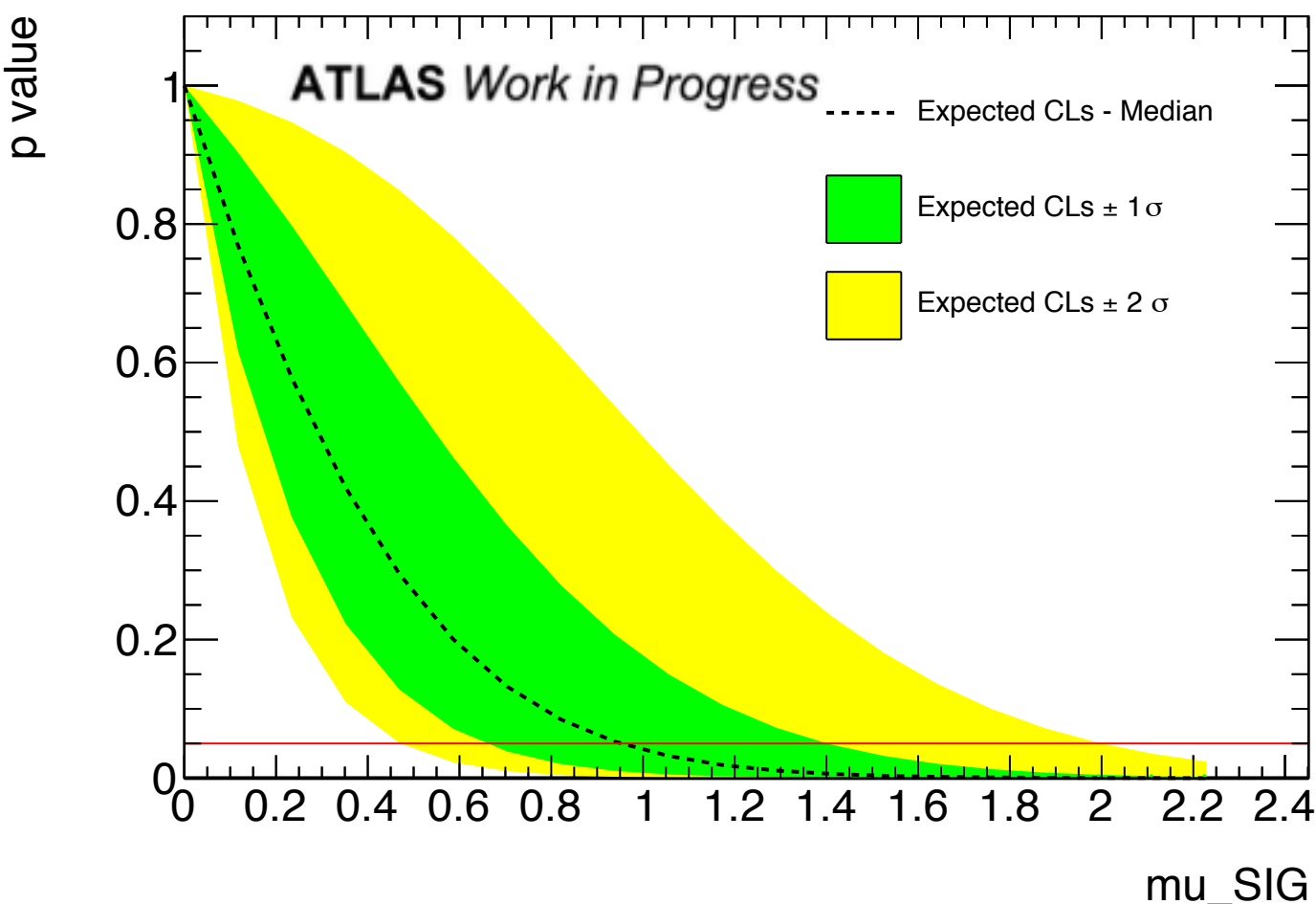
The most straightforward technique is the use of Boosted Decision Trees (BDTs).

TMVA is fed physics variables (m_{jj} , Δy_{jj} , m_{ll} , Δy_{ll} , $E_{T\text{miss}}$) and cuts in the variable space while considering correlation effects.

Extracting limits

Exclusion limits are extracted using the HistFitter software.

P-value: How likely it is that, given no signal, statistical fluctuations produced what is observed or more signal-like.



μ_{sig} : The strength of simulated signal present.

Cases above the line are excluded at a 95% confidence level.

Conclusion

- VBS is an ideal process to observe effects of fermiophobic extensions to the Higgs sector.
- Signal selection has been optimized. Will be further improved by the use of an MVA.
- Charge-flip is a major issue. A charge-flip killing tool (CFK) will be used to identify charge mis-ID.
- Pileup is an issue. A jet vertex tagging tool (fJVT) to be used to reduce pileup jets in the forward region.
- Limits to be extracted for a range of resonance masses.

Backup material

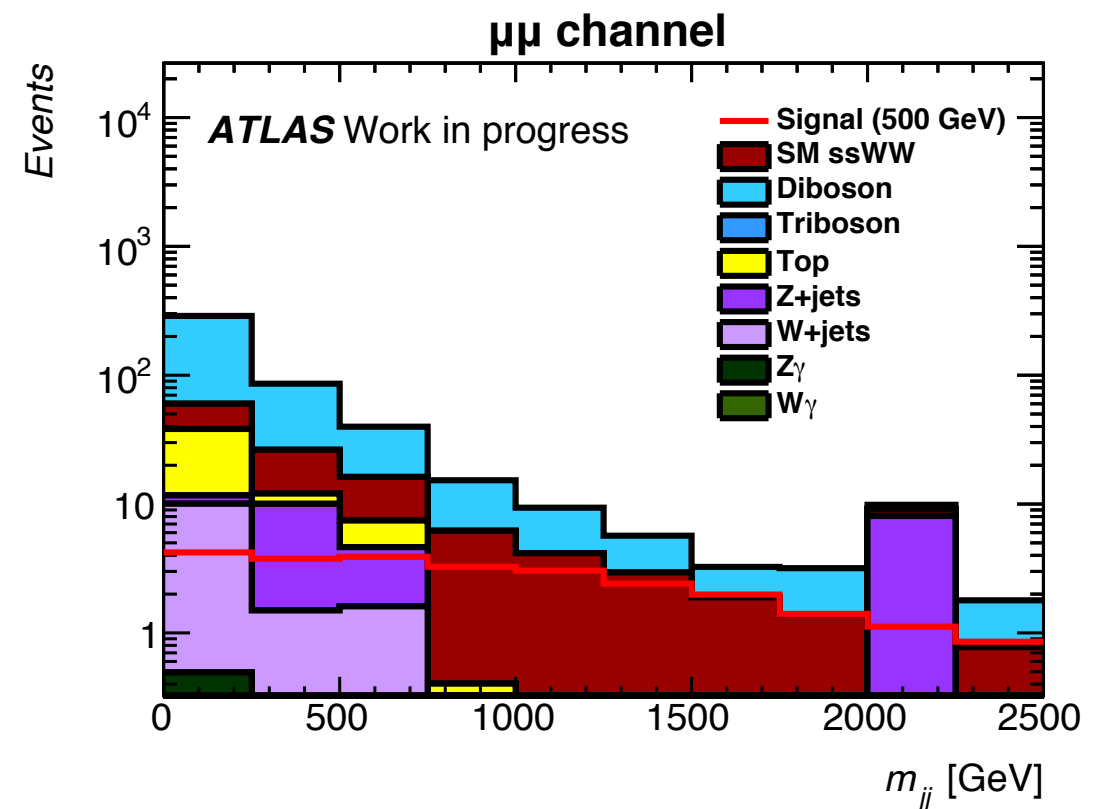
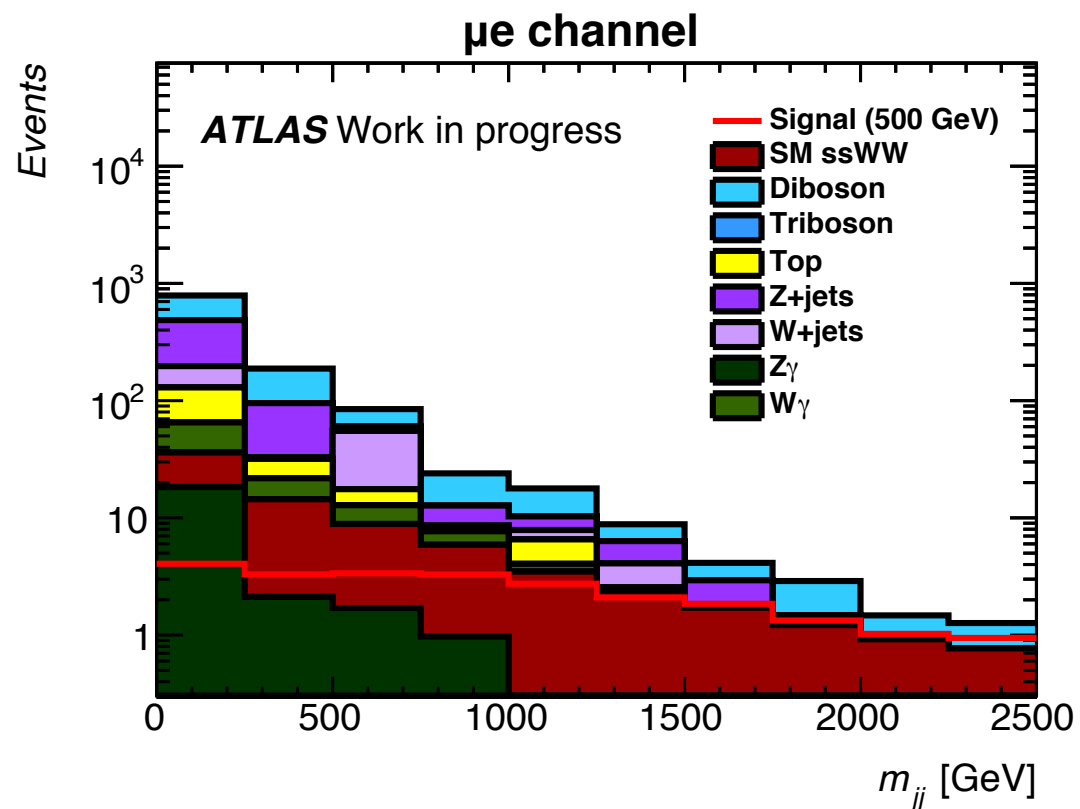
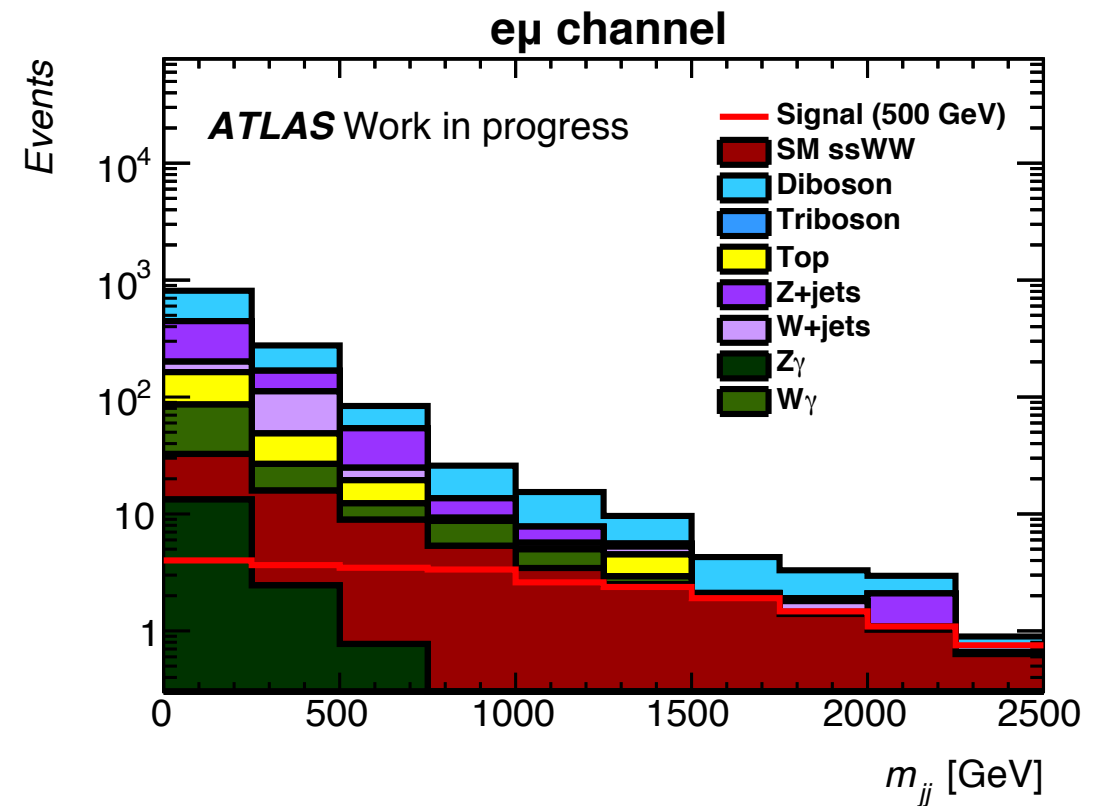
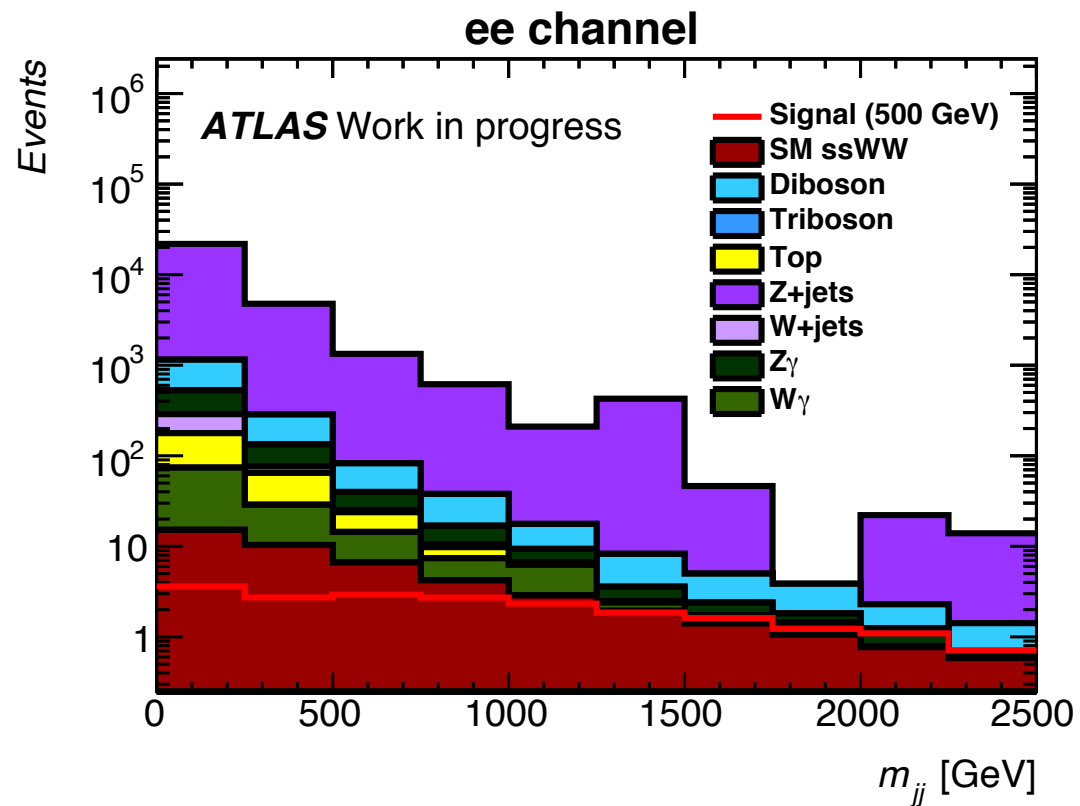
Generation of the signal samples

ATLAS searches for exotic particles use physics simulations as calculated by Monte-Carlo generators (here, MadGraph). These contain truth information, which is information about the physics process not available in data.

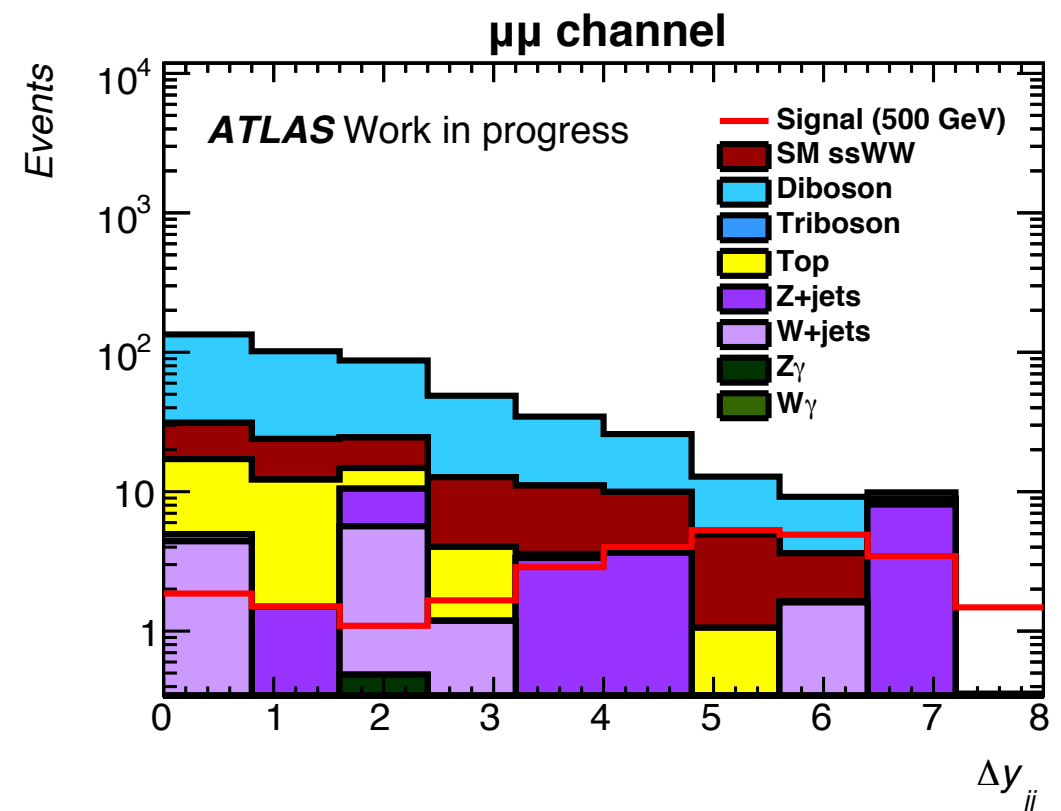
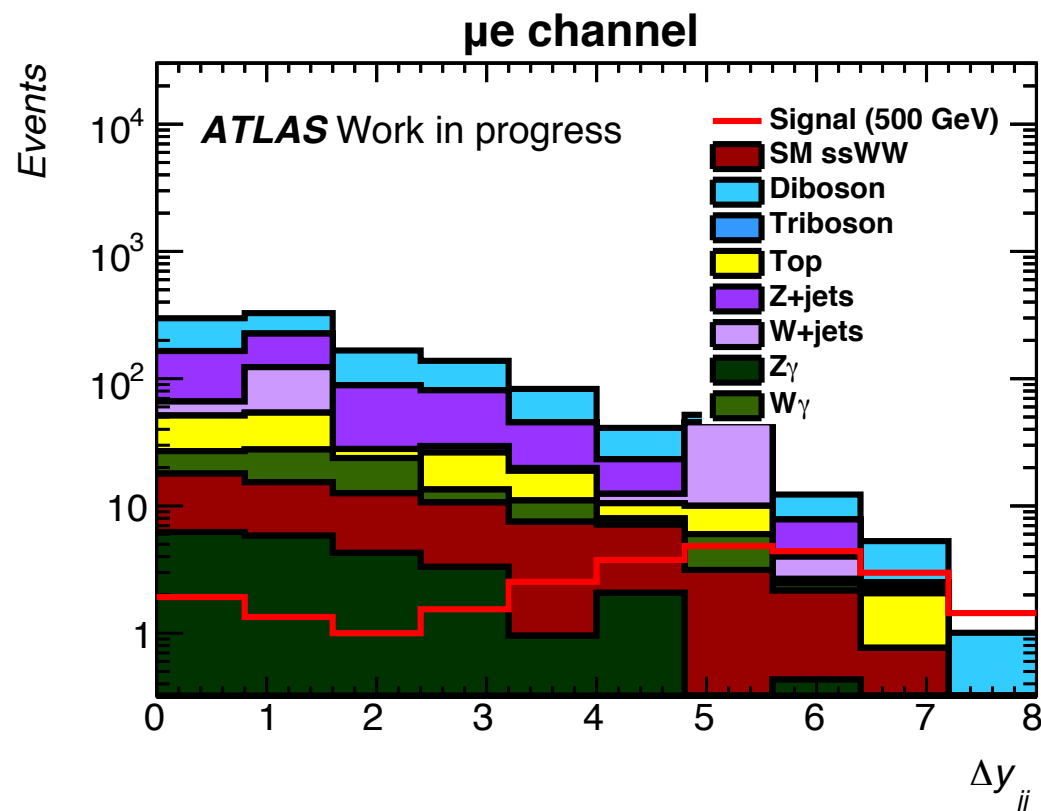
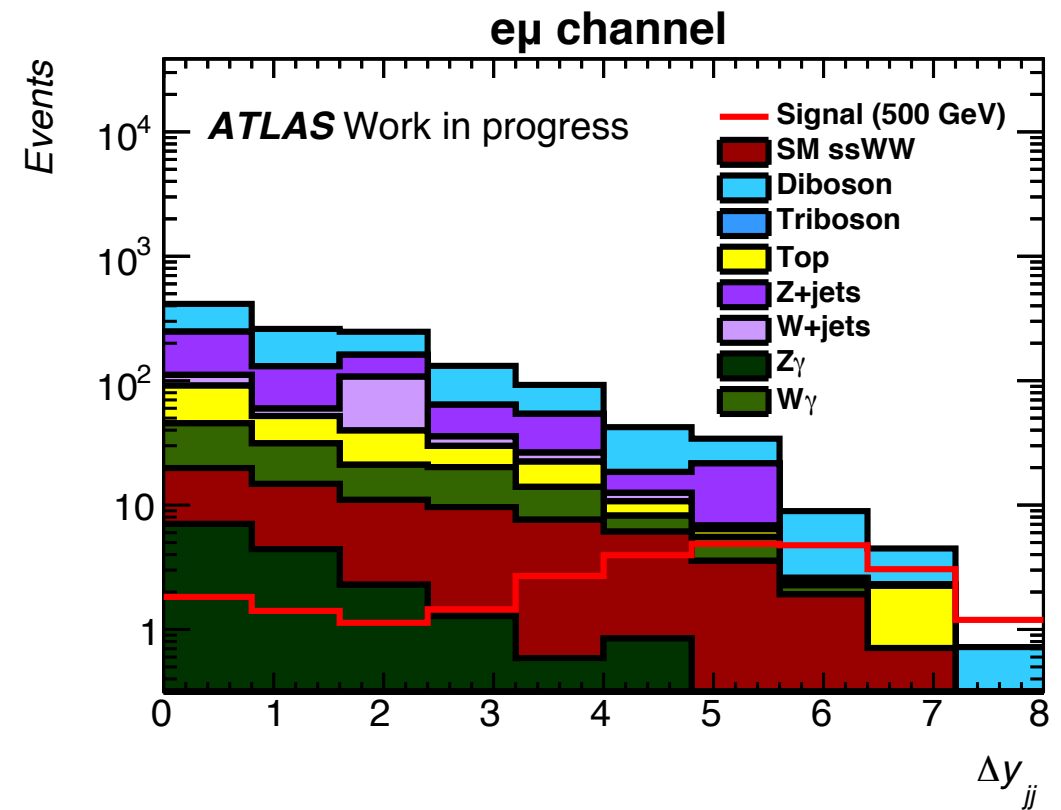
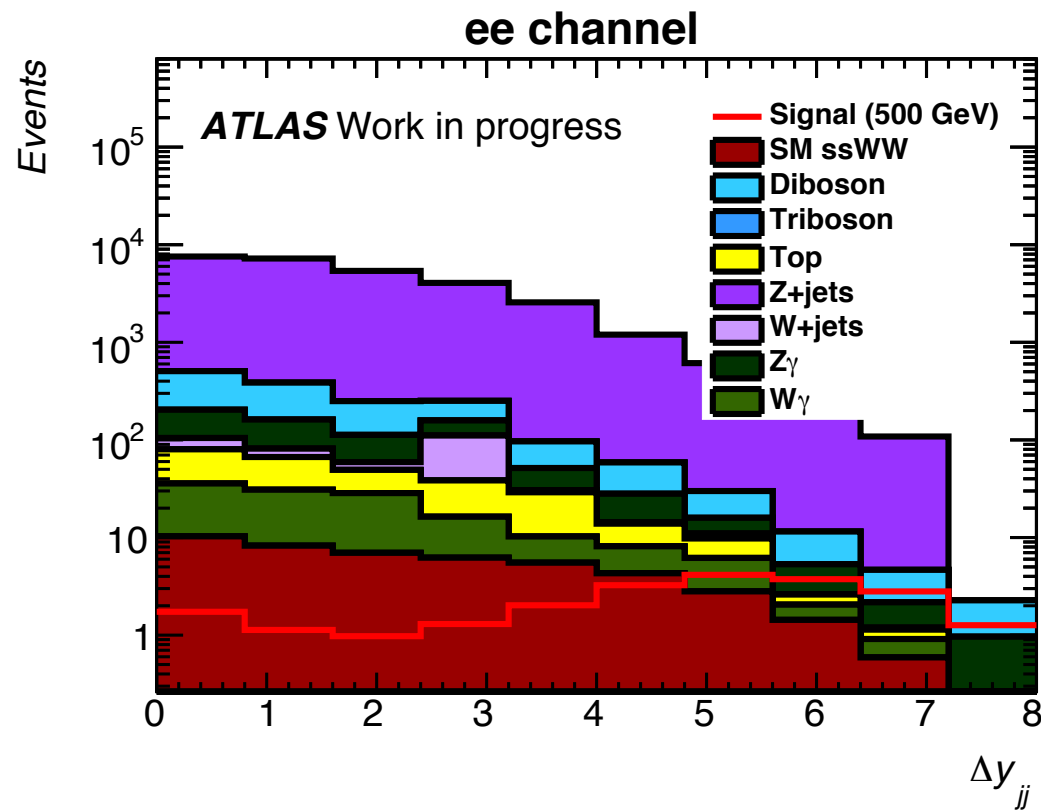
Physics simulation are then fed to a detector simulation (here, Geant4).

The simulated signal is extracted from this simulated background, and the effectiveness of this extraction can be checked using the truth information.

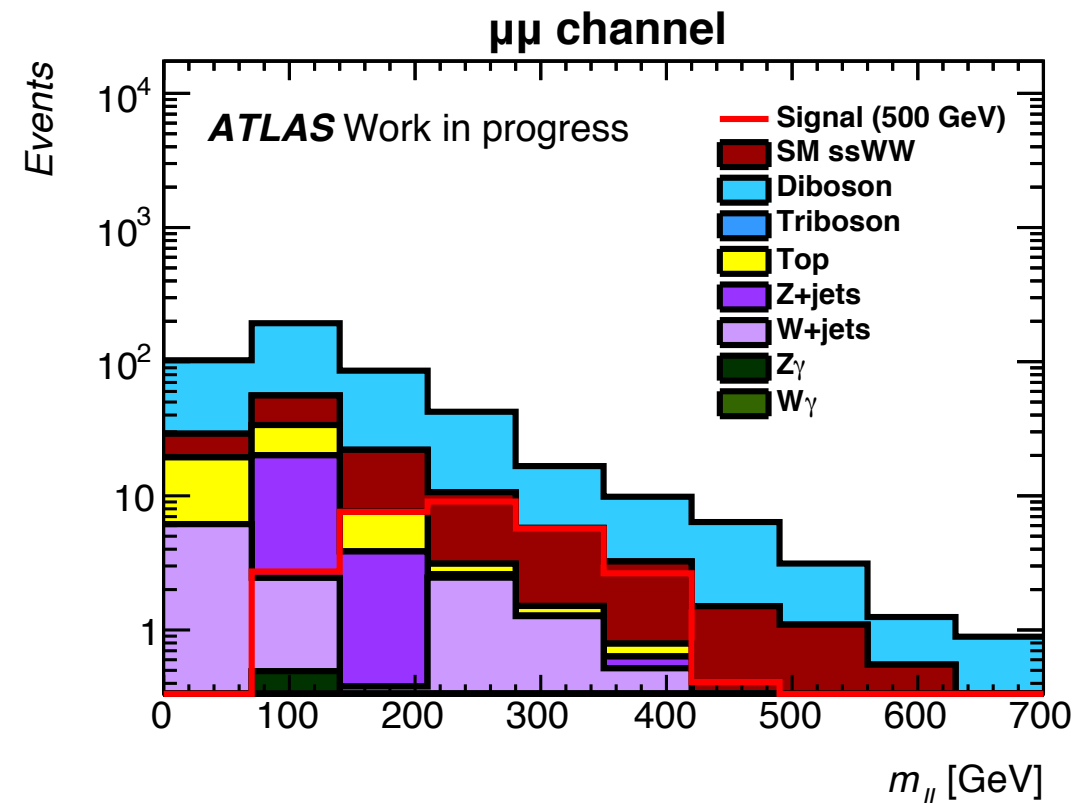
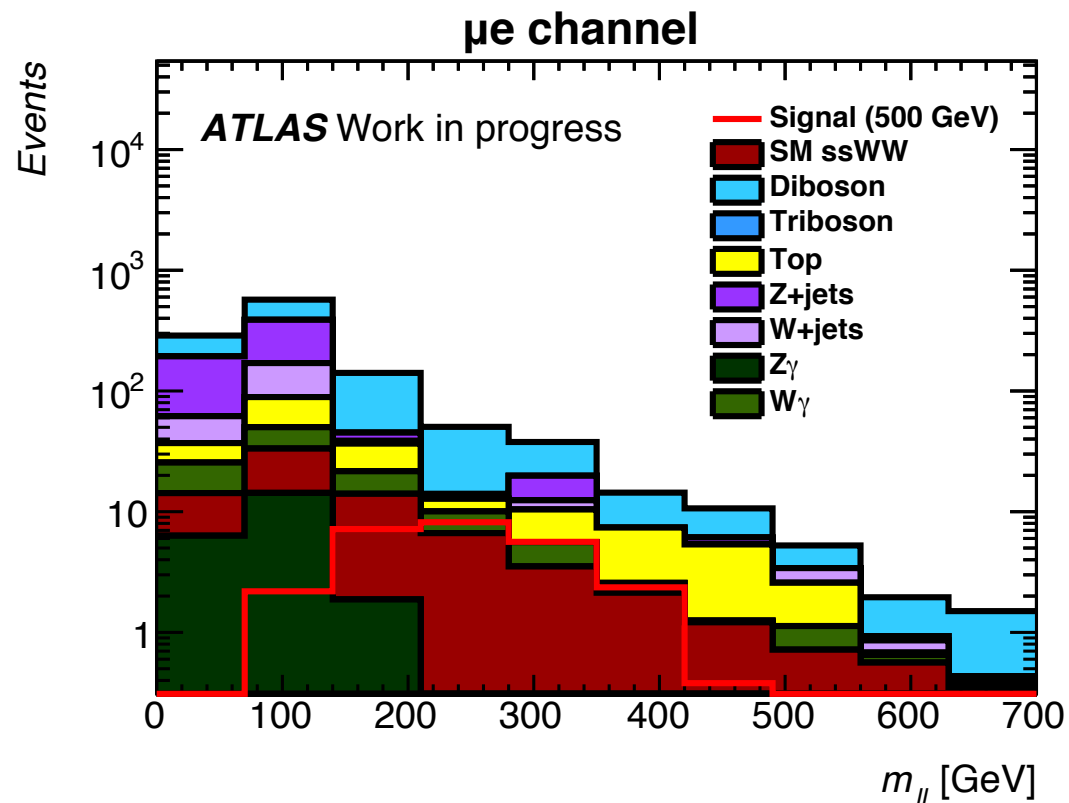
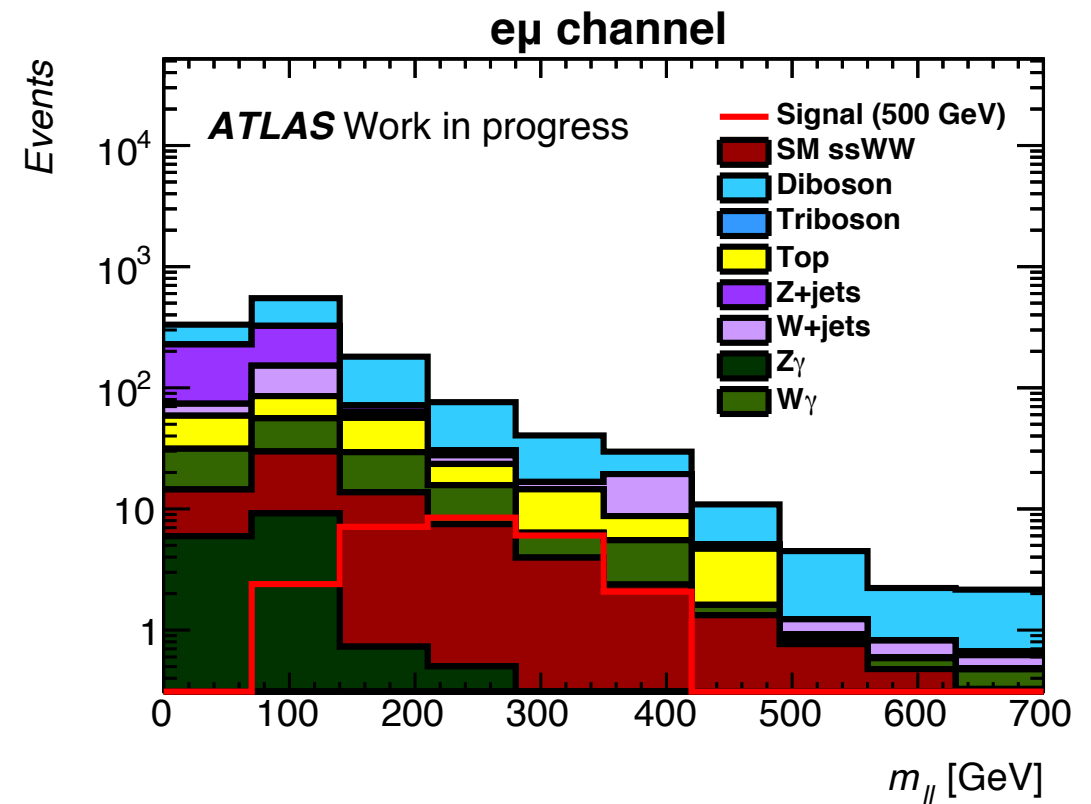
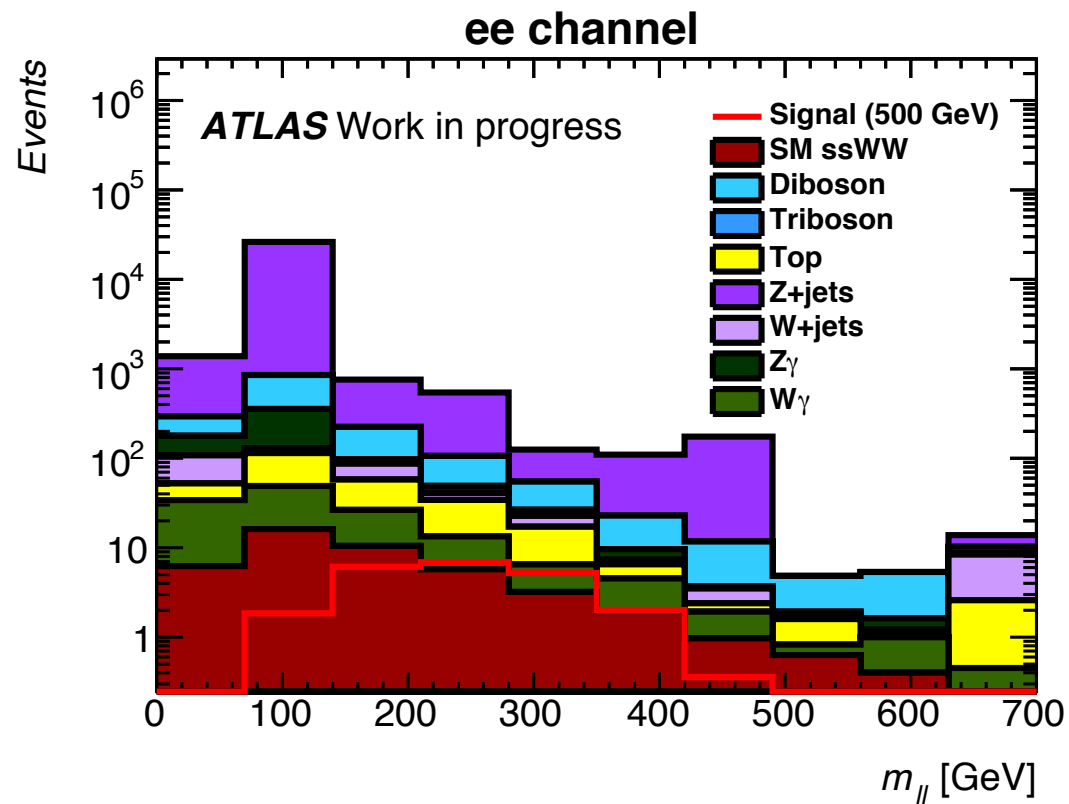
Background composition (m_{jj})



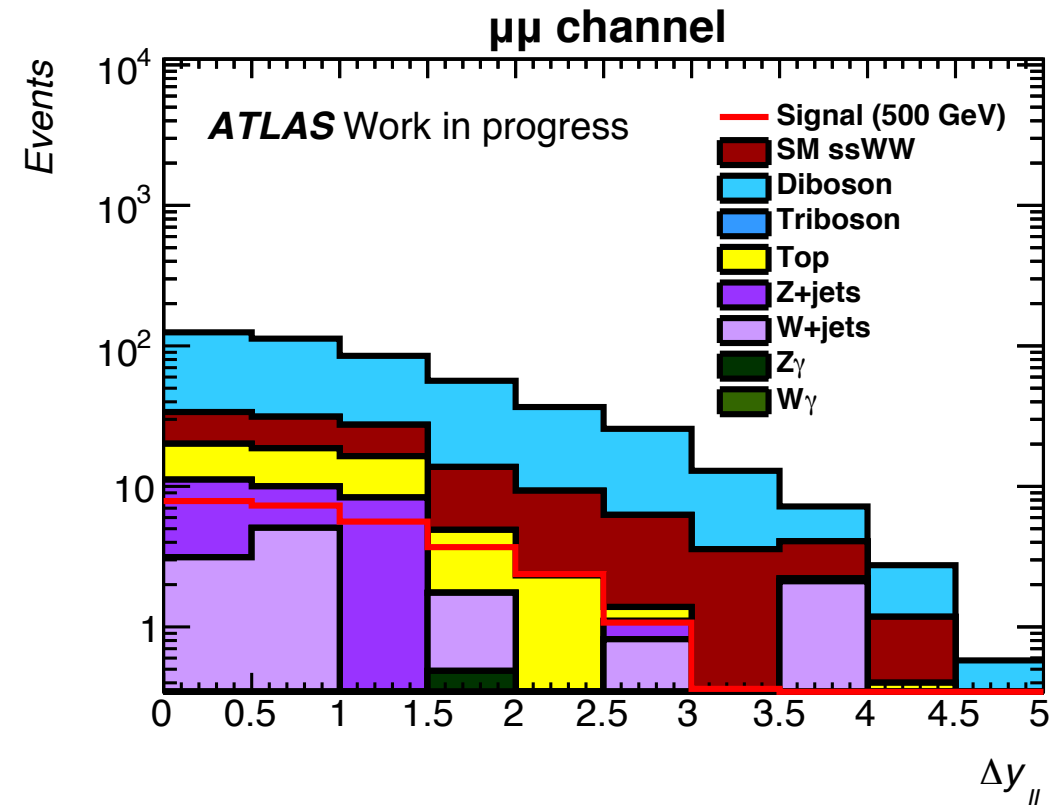
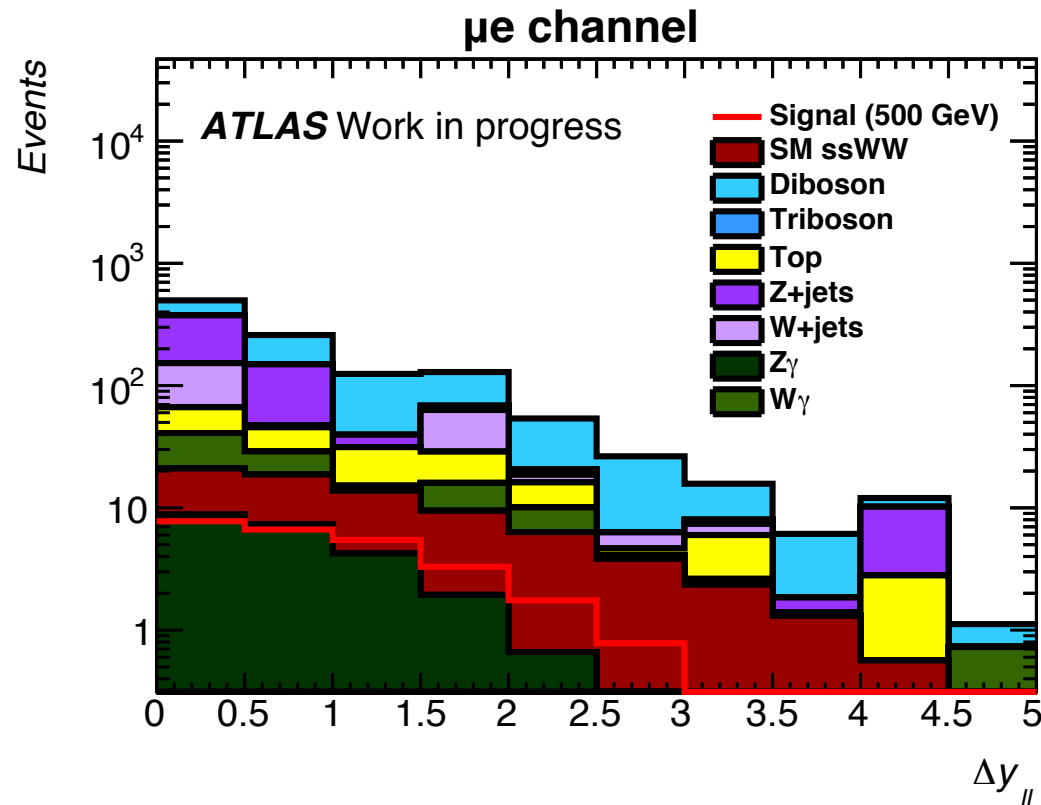
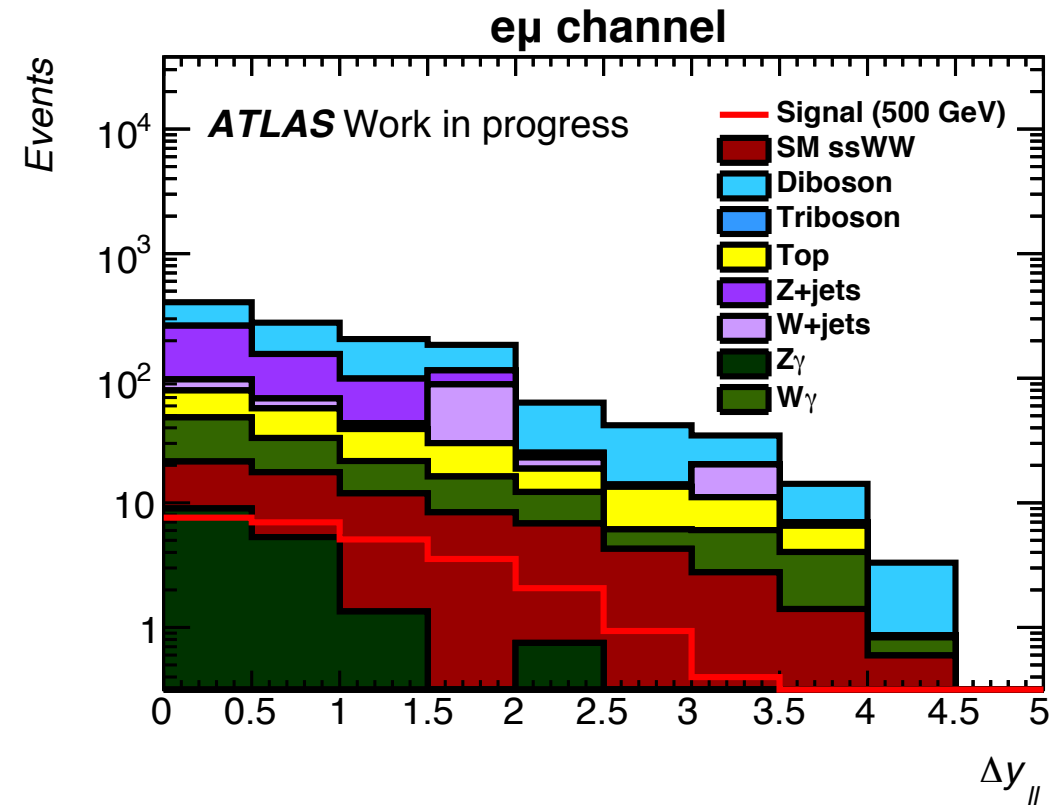
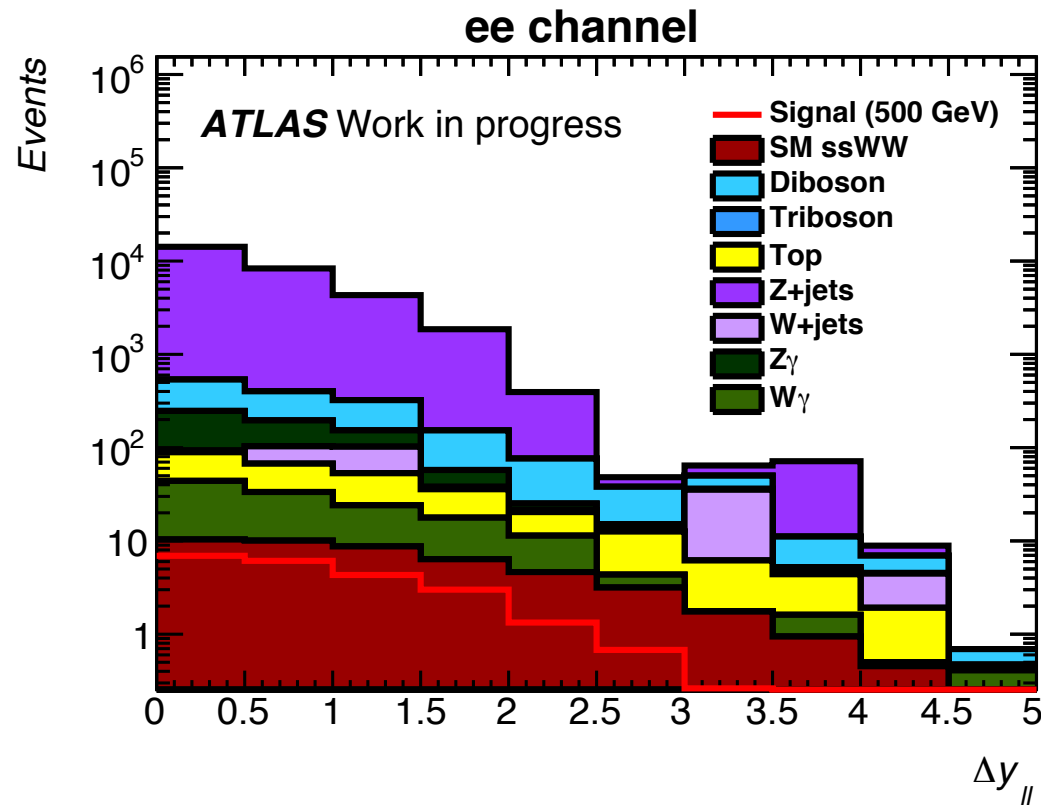
Background composition (Δy_{jj})



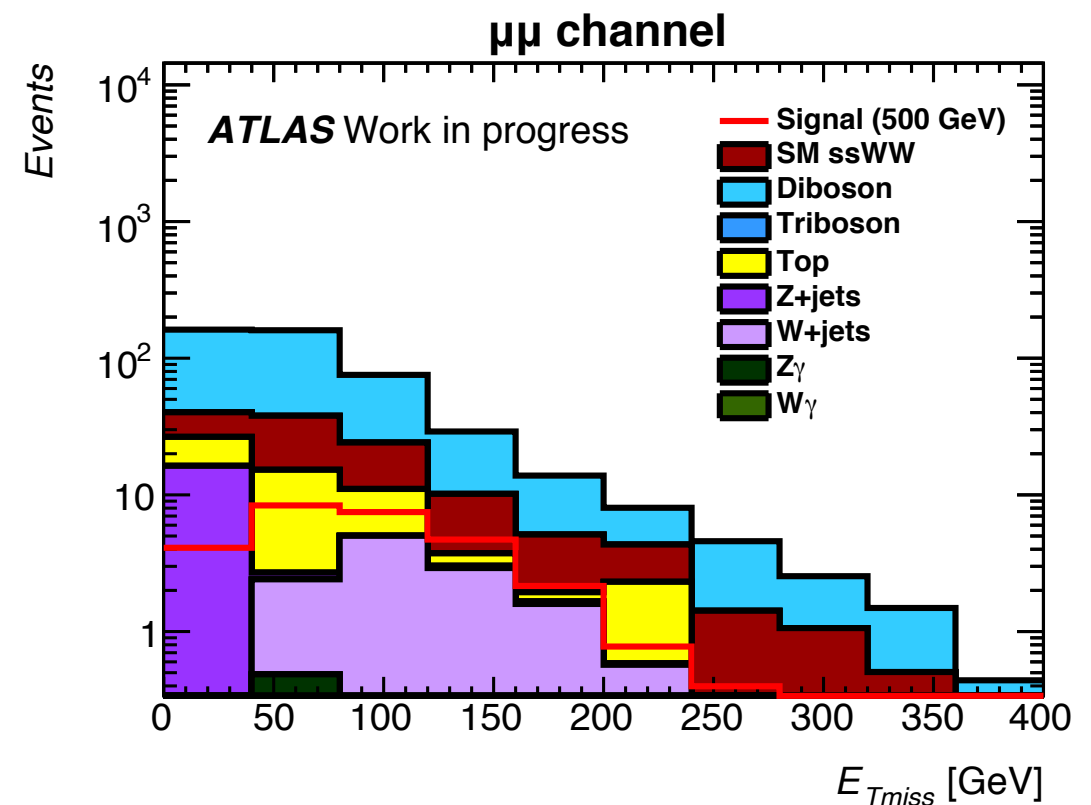
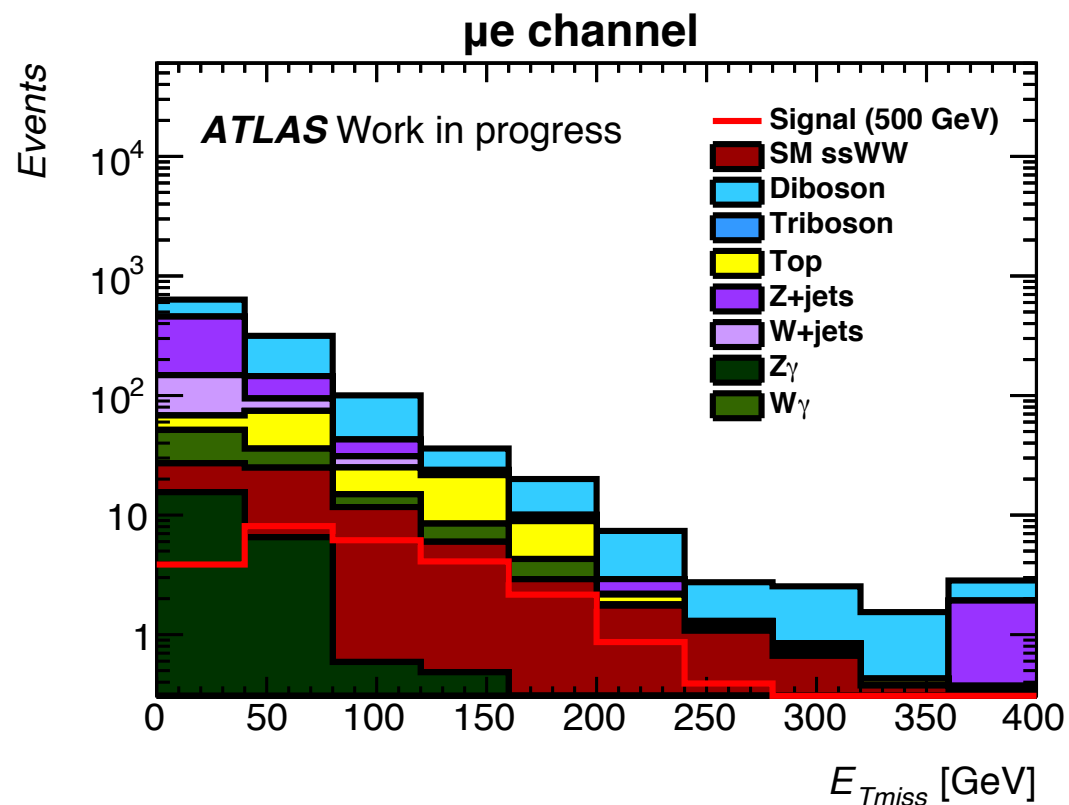
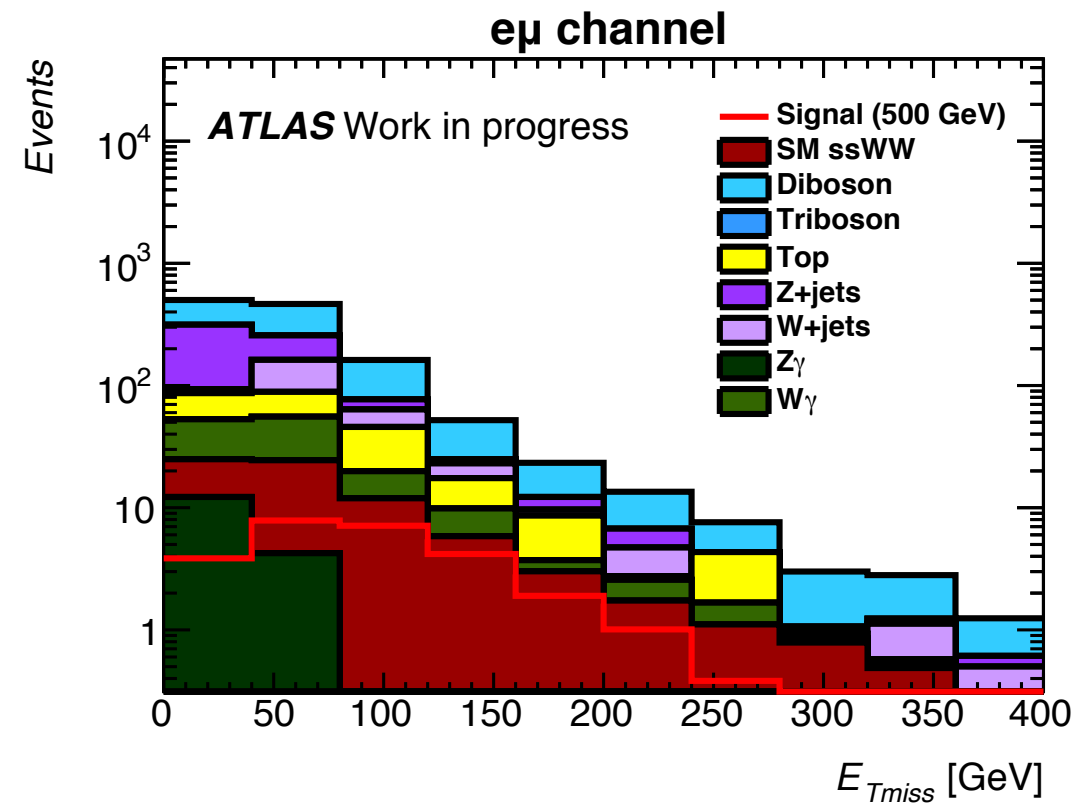
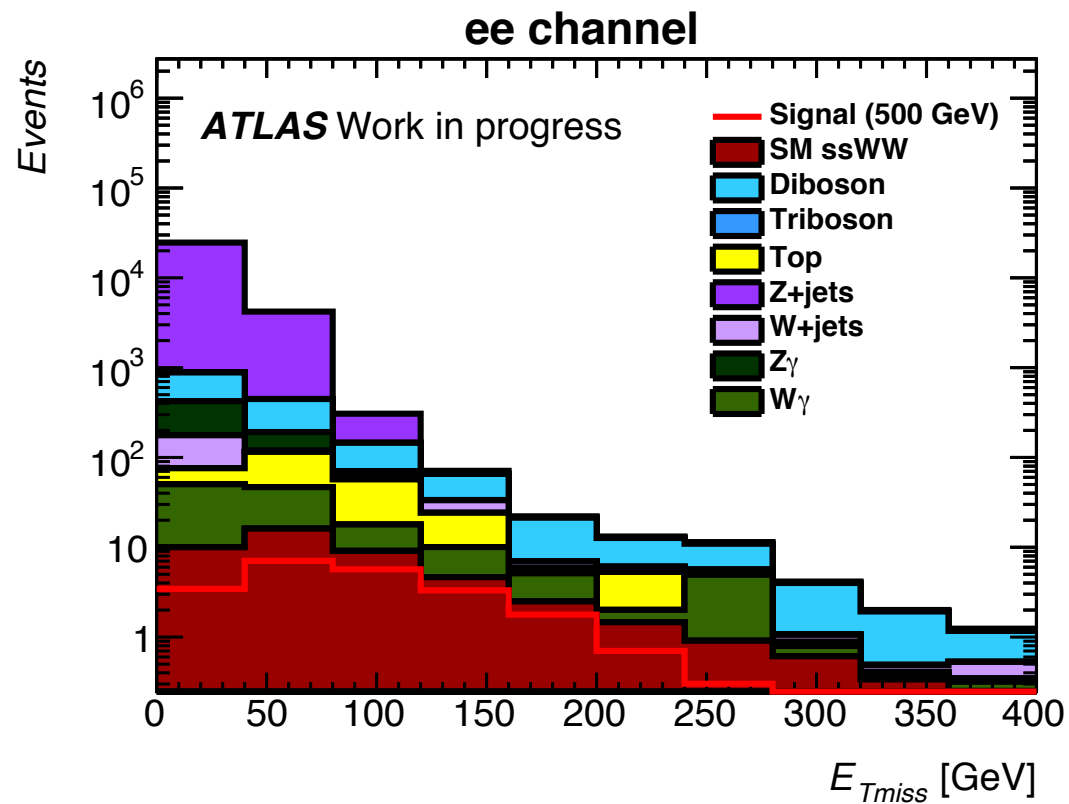
Background composition (m_{ll})



Background composition (Δy_{ll})



Background composition (E_{Tmiss})



Mass reconstruction

As with all resonance searches, we wish to reconstruct the mass of the resonance.

Because there are neutrinos (missing E_T) from both W decays, true mass reconstruction is not possible.

We also expect any sort of transverse mass reconstruction to worsen at high masses because of back-to-back neutrinos.

We explore several definitions of transverse mass as described by S. Todt in CERN-THESIS-2015-018.

Mass reconstruction

When projecting 4-momentum, the energy component can be defined in multiple ways:

- In a mass-preserving way:

$$e_{\top} \equiv \sqrt{M^2 + |\vec{p}_T|^2} = \sqrt{E^2 - p_z^2} \qquad p_{\top}^{\alpha} p_{\top\alpha} = m_{\top}^2 = M^2$$

- In a massless way:

$$e_o \equiv |\vec{p}_T| \qquad p_o^{\alpha} p_{o\alpha} = m_o = 0$$

Mass reconstruction

When reconstructing mass, the sum can be made before or after the projection. Three different definitions are possible:

- Sum first (mass-preserving):

$$m_{1T}^2 = \left(\sqrt{M_{ll}^2 + \vec{p}_{1T}^2} + E_T^{\text{miss}} \right)^2 - \left(\vec{p}_{1T} + \vec{E}_T^{\text{miss}} \right)^2$$

- Sum first (massless):

$$m_{1o}^2 = \left\{ |\vec{p}_{l_1T} + \vec{p}_{l_2T}| + E_T^{\text{miss}} \right\}^2 - \left(\vec{p}_{1T} + \vec{E}_T^{\text{miss}} \right)^2$$

- Sum last:

$$\begin{aligned} m_{T1}^2 &= \left(|\vec{p}_{l_1T}| + |\vec{p}_{l_2T}| + E_T^{\text{miss}} \right)^2 - \left(\vec{p}_{1T} + \vec{E}_T^{\text{miss}} \right)^2 \\ &= m_{o1}^2 \end{aligned}$$

Mass reconstruction

Other popular transverse mass variables:

- Visible mass:
$$\begin{aligned} m_{\text{vis}}^2 &\equiv M_{ll}^2 \\ &= (P_{l_1}^\mu + P_{l_2}^\mu)(P_{\mu l_1} + P_{\mu l_2}) \\ &= 2 \{ |\vec{p}_{l_1}| |\vec{p}_{l_2}| (1 - \cos \Delta\theta(l_1, l_2)) \} \end{aligned}$$

- Effective mass:
$$m_{\text{eff}}^2 = (|\vec{p}_{l_1 T}| + |\vec{p}_{l_2 T}| + E_T^{\text{miss}})^2$$

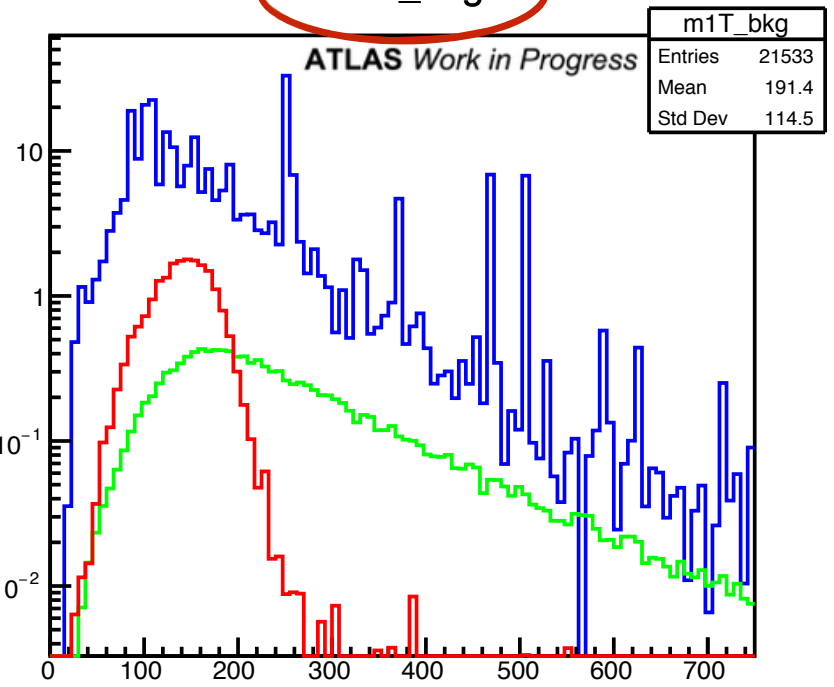
- Vectorial mass:

$$\begin{aligned} m_{\text{vec}}^2 &= (P_{l_1}^\mu + P_{l_2}^\mu + P^{\mu \text{miss}})(P_{\mu l_1} + P_{\mu l_2} + P_{\mu}^{\text{miss}}) \\ &= (|\vec{p}_{l_1}| + |\vec{p}_{l_2}| + E_T^{\text{miss}})^2 - \left(\vec{p}_{l_1 T} + \vec{p}_{l_2 T} + \vec{E}_T^{\text{miss}} \right)^2 - (p_{l_1 z} + p_{l_2 z})^2 \end{aligned}$$

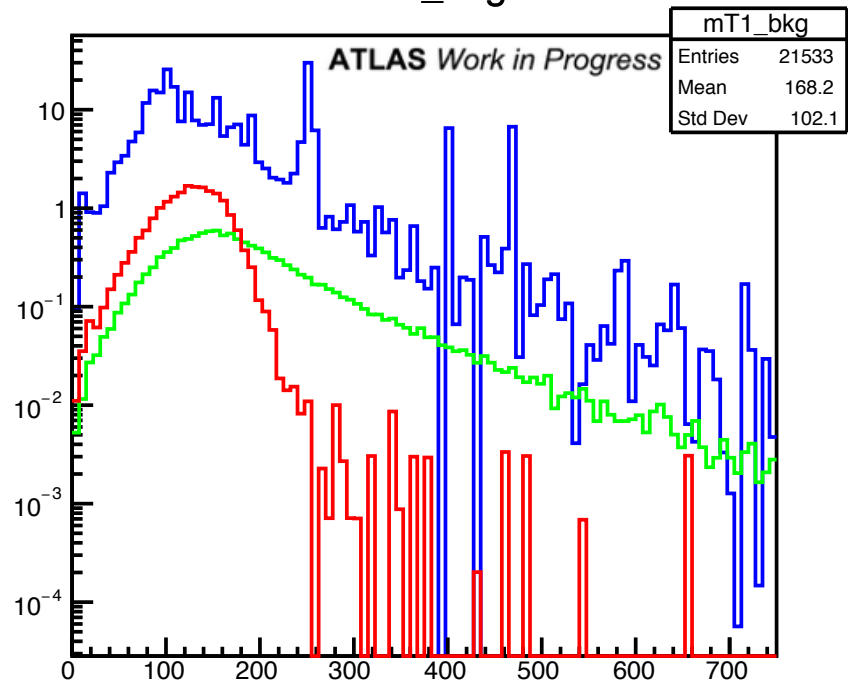
$$P_{\mu}^{\text{miss}} = \left(E_T^{\text{miss}}, \vec{E}_T^{\text{miss}}, 0 \right)$$

Mass reconstruction (200 GeV)

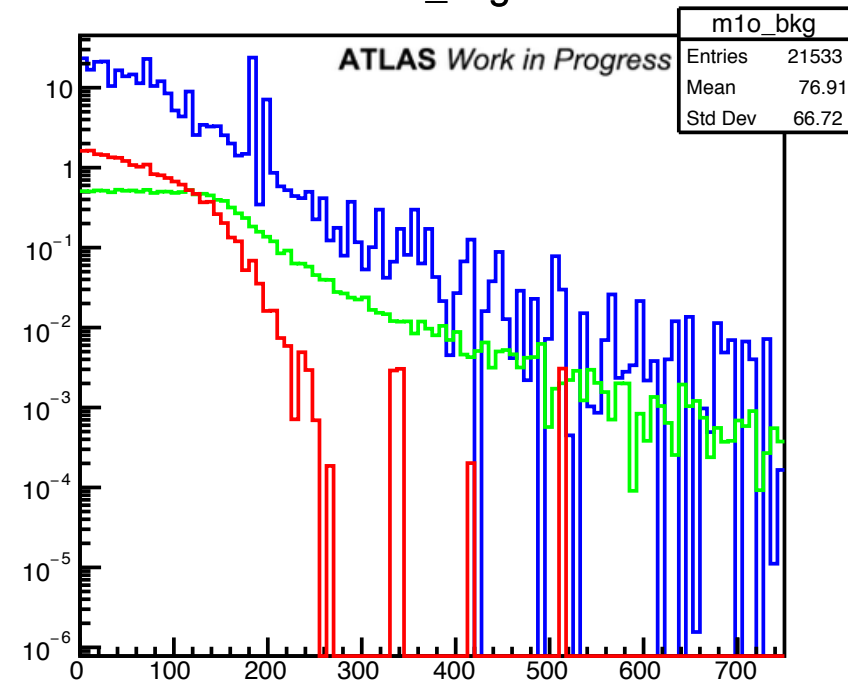
m1T_bkg



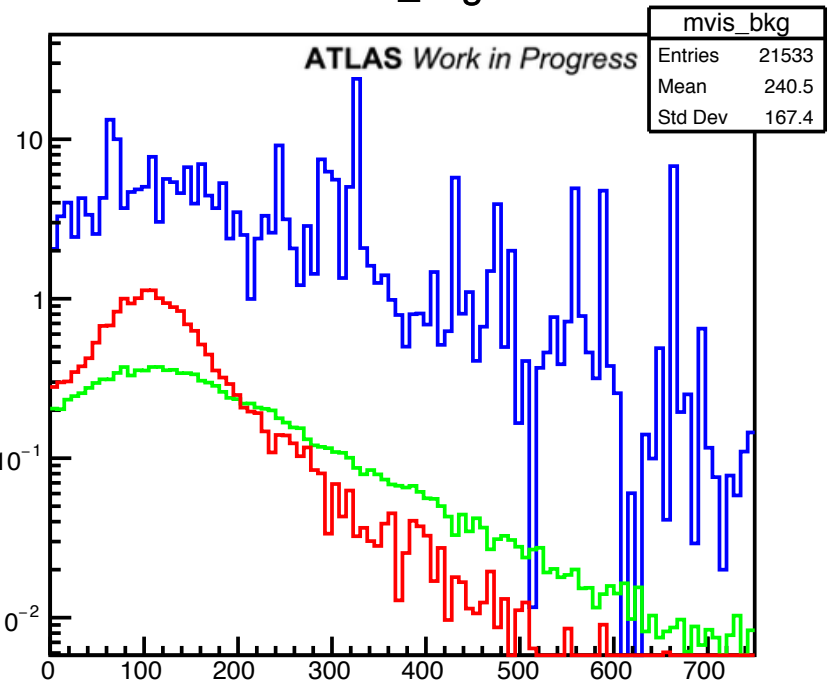
mT1_bkg



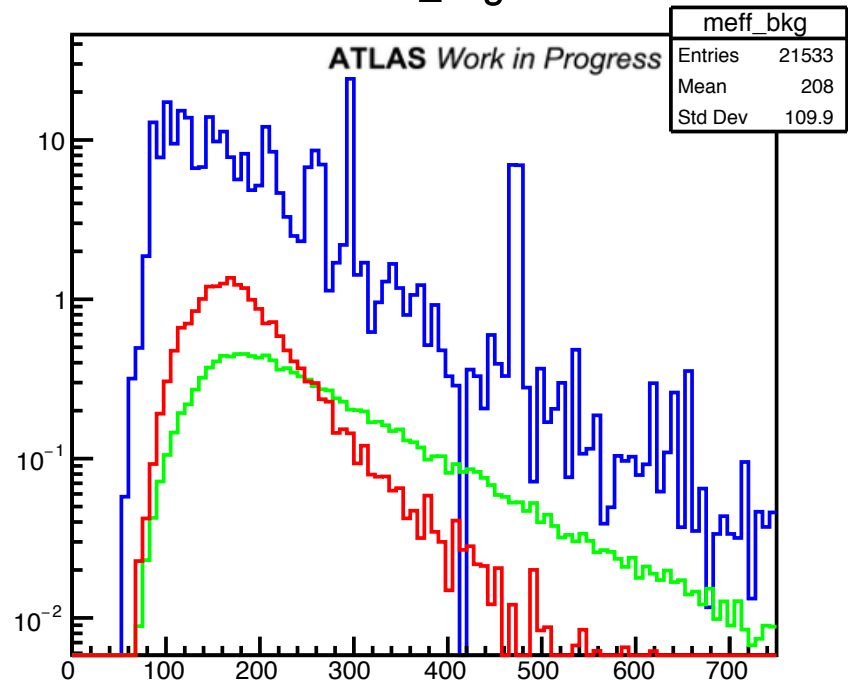
m1o_bkg



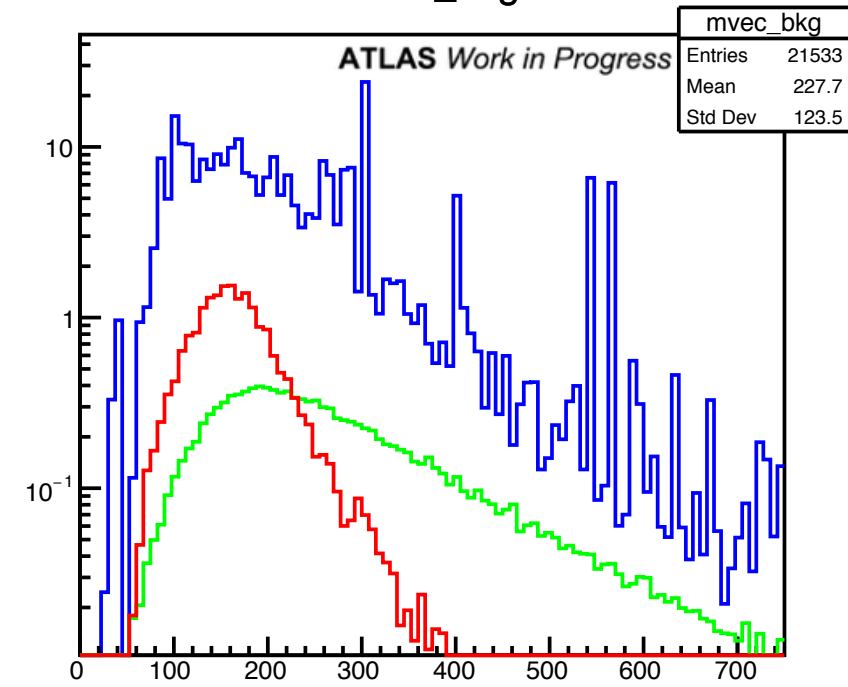
mvis_bkg



meff_bkg



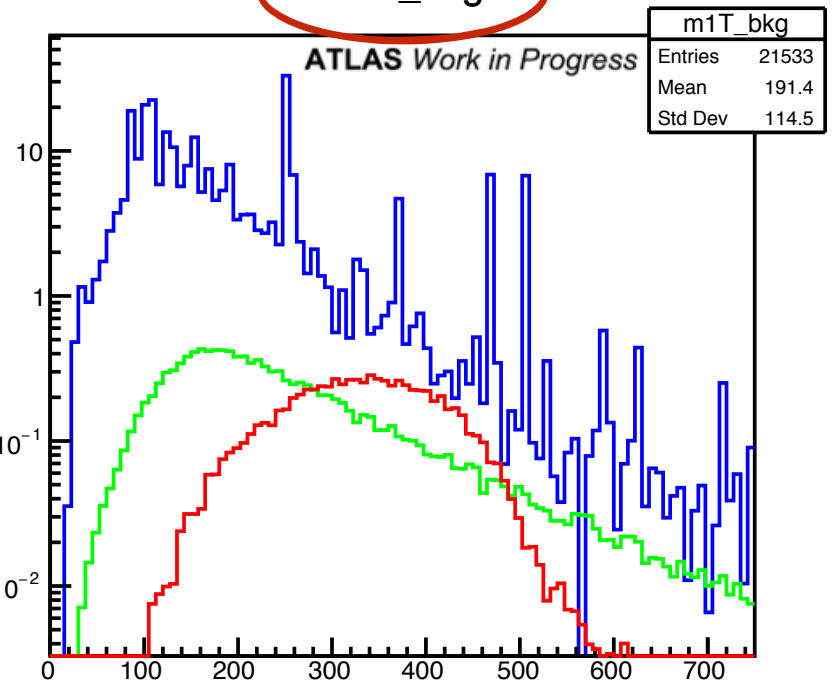
mvec_bkg



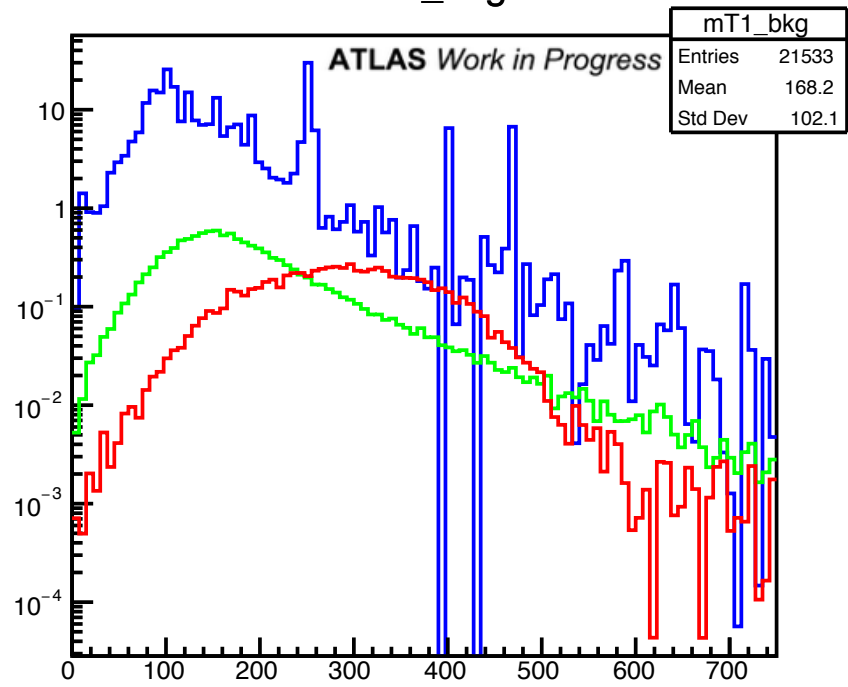
BSM SIG **SM BKG** **Mis-ID**

Mass reconstruction (500 GeV)

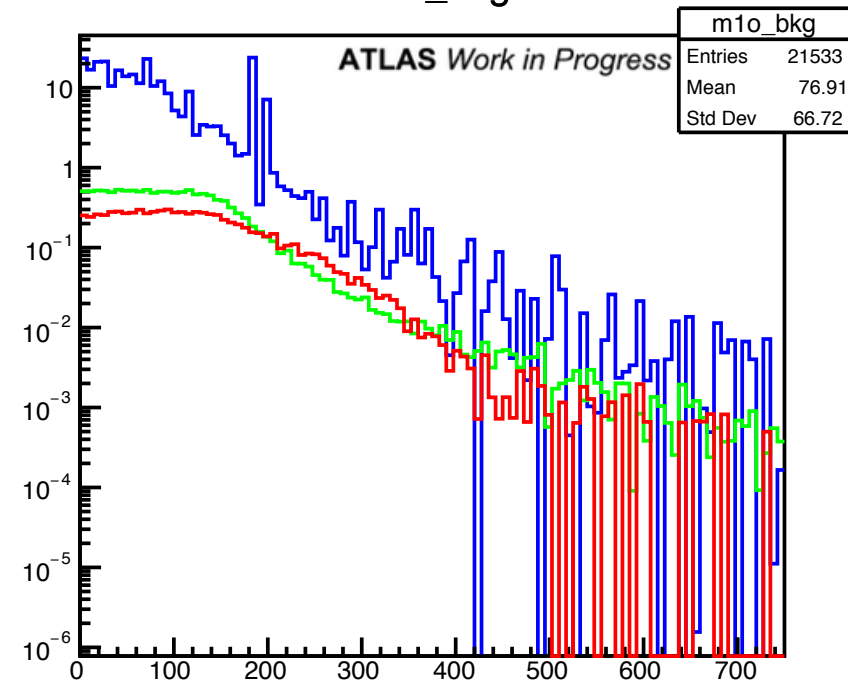
m1T_bkg



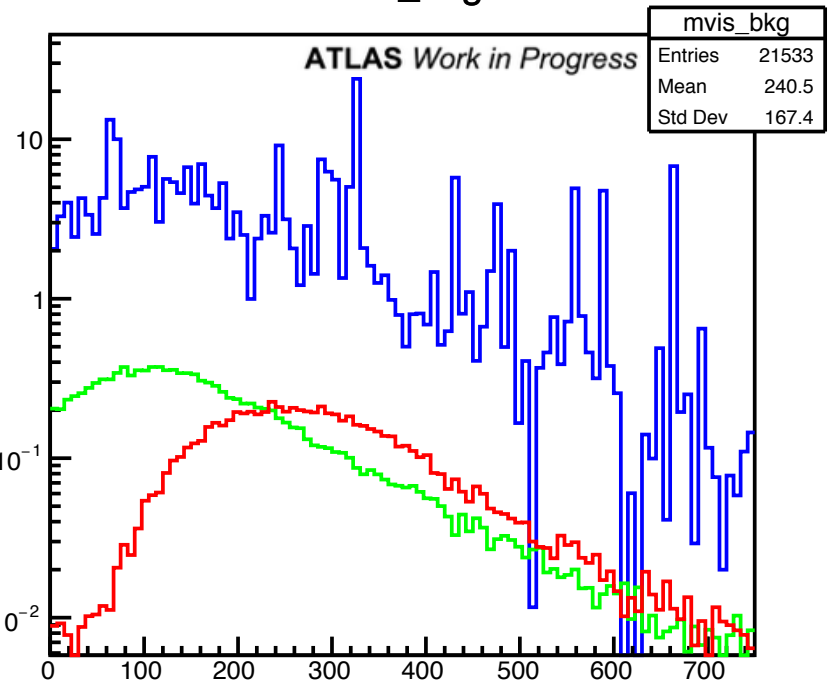
mT1_bkg



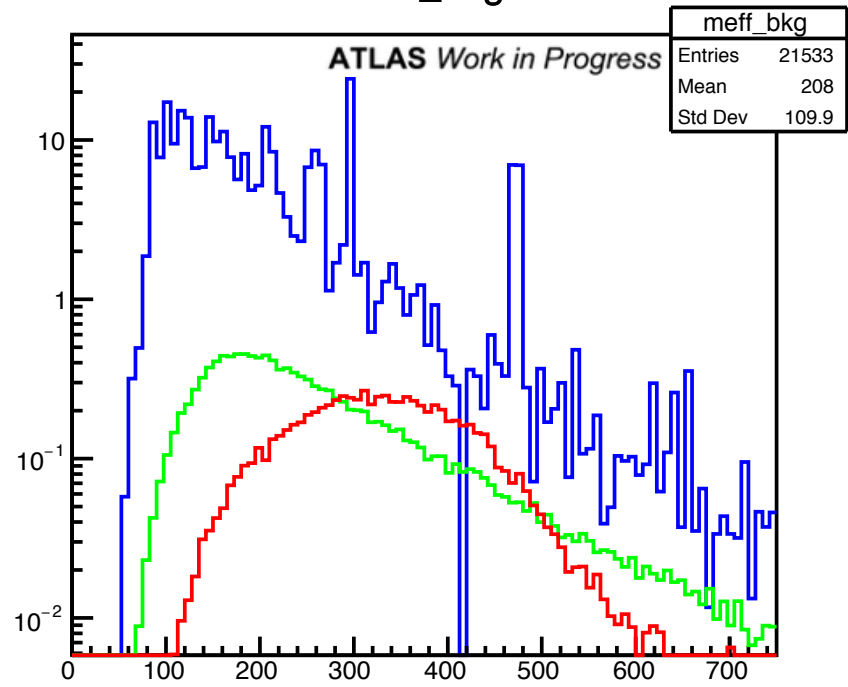
m1o_bkg



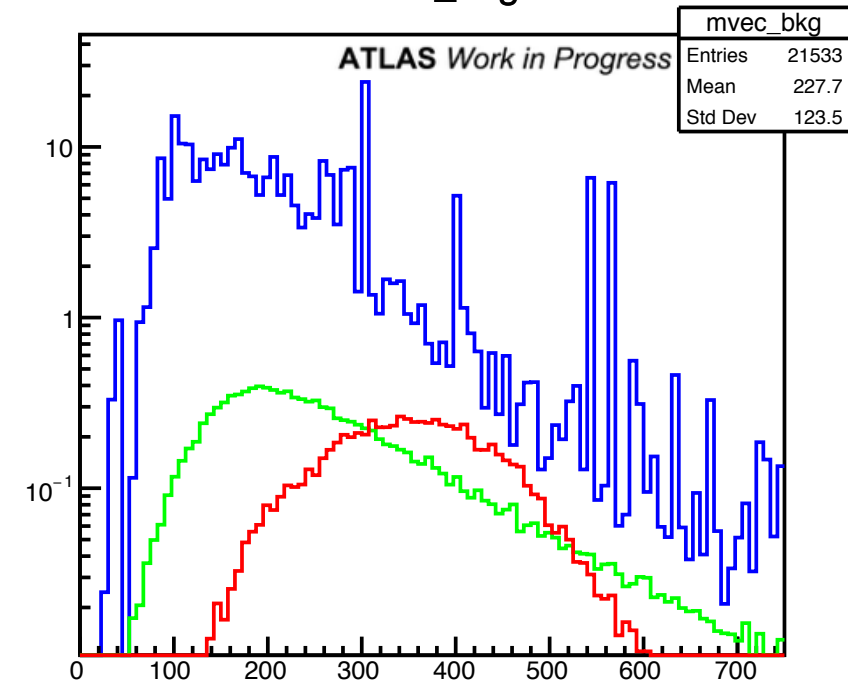
mvis_bkg



meff_bkg

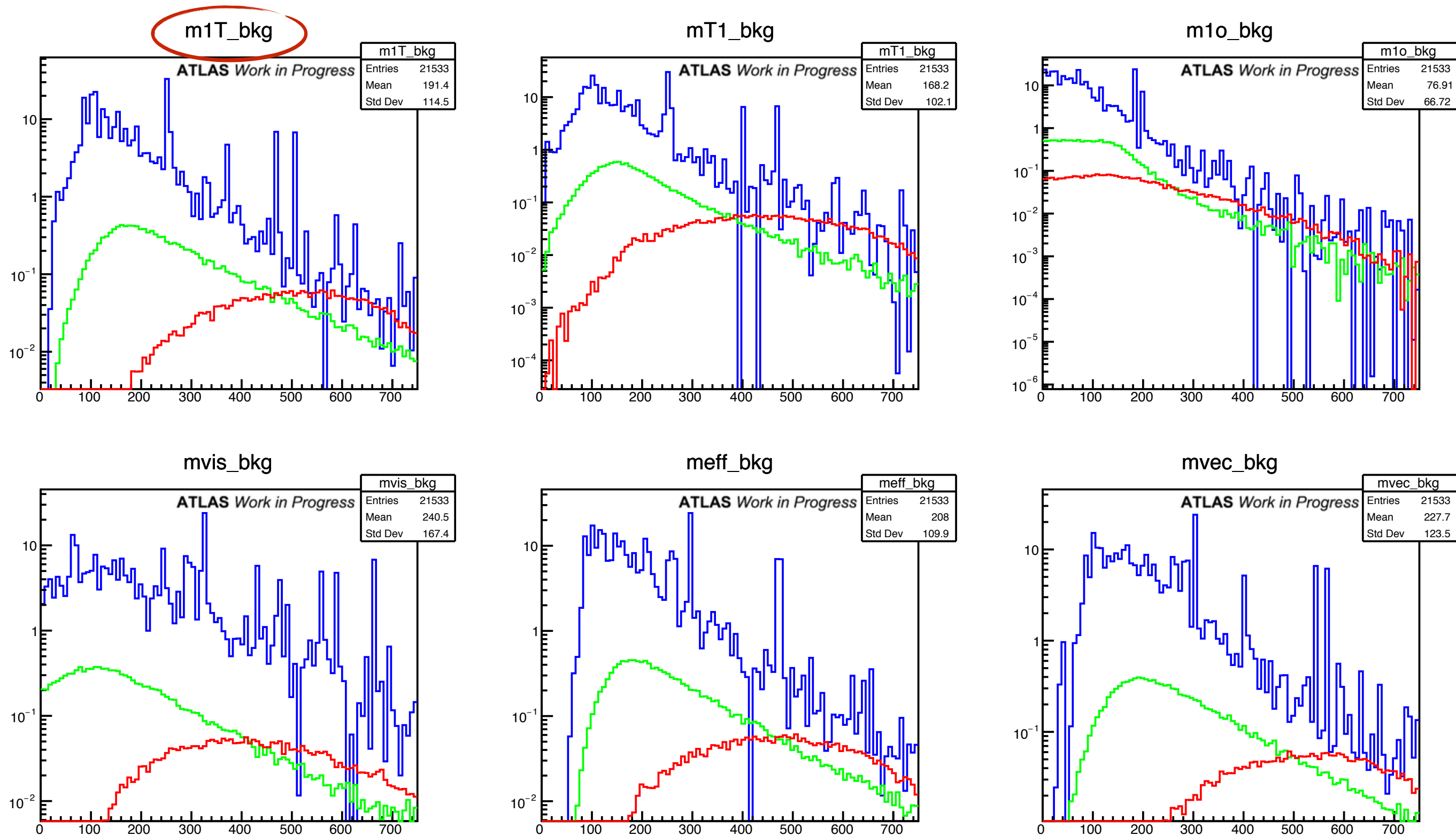


mvec_bkg



BSM SIG **SM BKG** **Mis-ID**

Mass reconstruction (800 GeV)



BSM SIG **SM BKG** **Mis-ID**

Square cut optimization

The following table outlines the 5D grid used for the optimization:

Cut	Min	Max	Step
m_{jj} (GeV)	200	600	50
Δy_{jj}	1	9	1
m_{ll} (GeV)	0	300	100
Δy_{ll}	1	6	1
$E_{T\text{miss}}$ (GeV)	10	80	10

Aside from Δy_{ll} , these are lower-bound cuts.

Square cut optimization results

For $\mu\mu$ and $e\mu/\mu e$ channels:

- High m_{jj} cut, high jet separation (VBS jets)
- m_{ll} increasing with resonance mass and low lepton separation (from the resonance decay)
- No use for an $E_{T\text{miss}}$ cut (not discriminant)

Higher significance for lower resonance masses (from 7.5 to 3). Similar amounts of signal and background.

Square cut optimization results

For **ee** channel: two regimes.

400 GeV and under:

- Higher m_{jj}
- High lepton separation
- Large E_{Tmiss} cuts

500 GeV and over:

- Higher m_{ll}
- Low lepton separation
- Moderate E_{Tmiss} at lower masses

Lower significance throughout (4 to 3.5). Some regimes with high background, others comparable.

Square cuts – ee channel

Results are chosen to maximize significance while minimizing wild changes with respect to mass.

Cut	Truth resonance mass (GeV)							
	200	300	400	500	600	700	800	900
m_{jj}	600	600	600	500	500	500	500	500
Δy_{jj}	5	6	6	5	5	5	5	5
m_{ll}	0	50	50	200	200	250	250	250
Δy_{ll}	6	6	6	2	2	2	2	2
E_{Tmiss}	50	50	50	30	30	10	10	10
#	20	1	1	19	15	15	2	7
σ	3.63	4.14	3.67	3.78	3.97	3.73	3.83	3.51
Signal	14.6	3.88	4.44	5.72	5.46	3.93	3.46	2.70
Bkg.	336	2.56	2.56	1.68	1.68	5.22	5.22	5.22

Square cuts – $e\mu/\mu e$ channel

Results are chosen to maximize significance while minimizing wild changes with respect to mass.

Cut	Truth resonance mass (GeV)							
	200	300	400	500	600	700	800	900
m_{jj}	400	500	500	500	500	500	500	500
Δy_{jj}	3	4	5	5	5	5	6	6
m_{ll}	50	50	100	150	150	150	150	150
Δy_{ll}	2	2	2	2	2	2	3	3
E_{Tmiss}	10	10	10	10	10	10	10	10
#	9	4	5	1	8	28	22	27
σ	7.70	6.64	6.57	6.59	6.07	5.35	4.95	4.32
Signal	72.7	49.9	26.9	19.1	15.4	12.3	5.86	4.55
Bkg.	128	75.9	19.6	8.26	8.26	8.26	2.65	2.65

Square cuts – $\mu\mu$ channel

Results are chosen to maximize significance while minimizing wild changes with respect to mass.

Cut	Truth resonance mass (GeV)							
	200	300	400	500	600	700	800	900
m_{jj}	400	500	500	500	500	500	500	500
Δy_{jj}	3	4	5	5	5	5	5	5
m_{ll}	50	50	50	50	150	150	150	150
Δy_{ll}	2	2	2	2	2	2	3	3
E_{Tmiss}	10	10	10	10	10	10	10	10
#	5	1	1	1	47	234	2	4
σ	7.76	6.23	5.28	4.76	3.84	3.56	3.35	3.12
Signal	45.3	30.4	16.4	13.0	8.50	6.77	5.48	4.10
Bkg.	42.2	25.5	12.1	12.1	4.18	4.18	5.17	5.17

TMVA results

The optimization yields can be compared to the square cut method.

		Resonance mass (GeV)							
Channel	Value	200	300	400	500	600	700	800	900
ee	σ								
	Signal								
	Bkg.								
e μ	σ								
	Signal			To be filled					
	Bkg.								
μ e	σ								
	Signal								
	Bkg.								
$\mu\mu$	σ								
	Signal								
	Bkg.								

Negative weights and TMVA

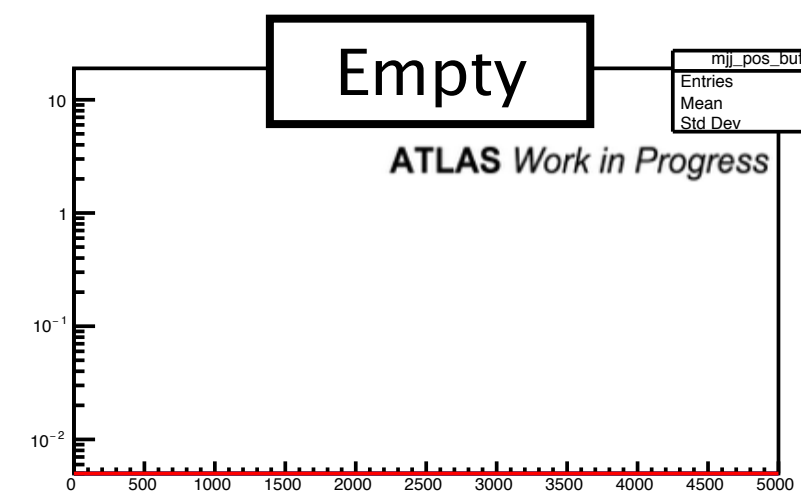
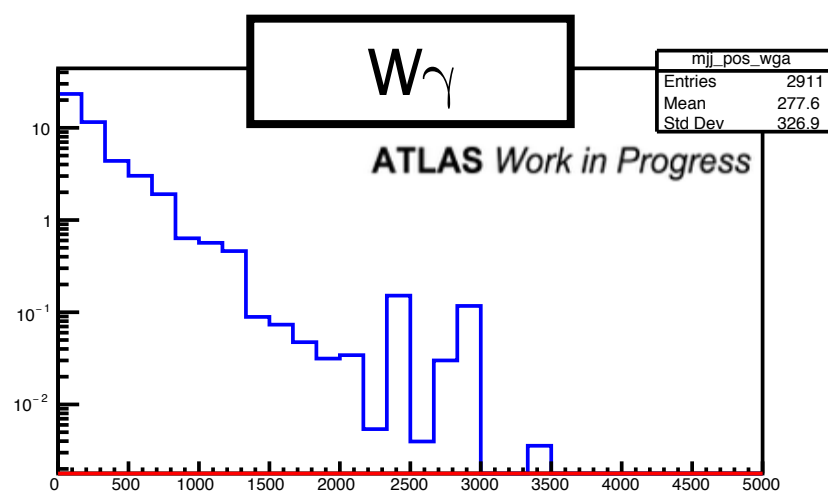
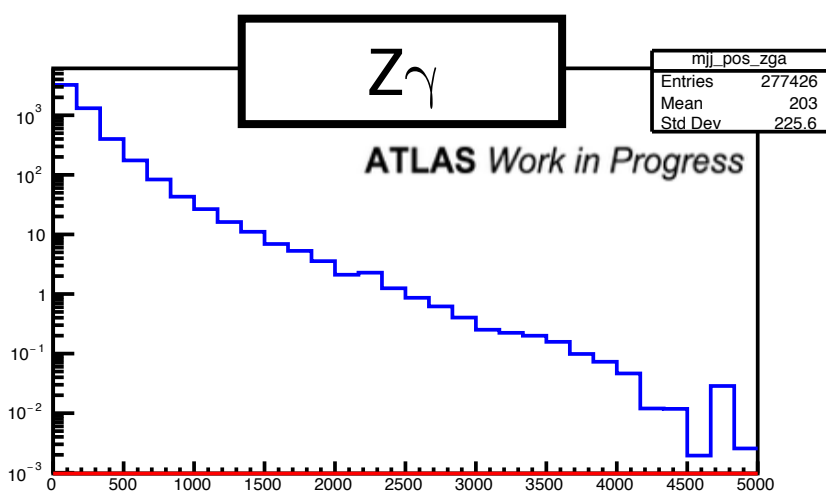
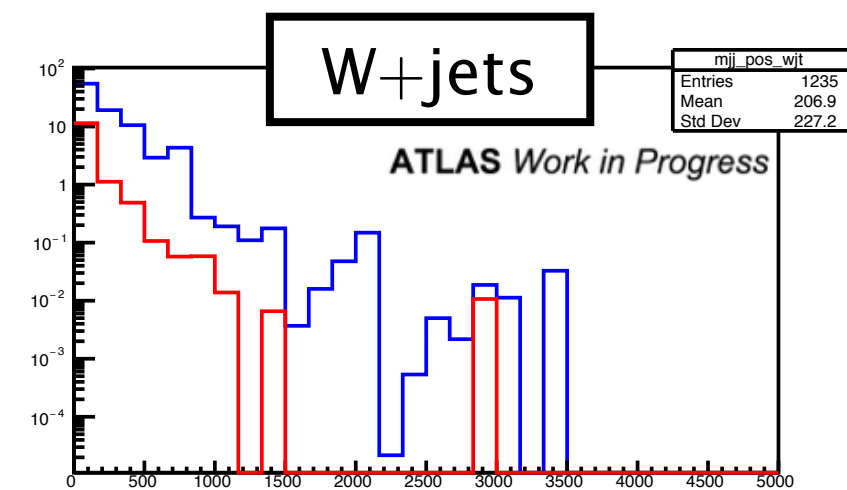
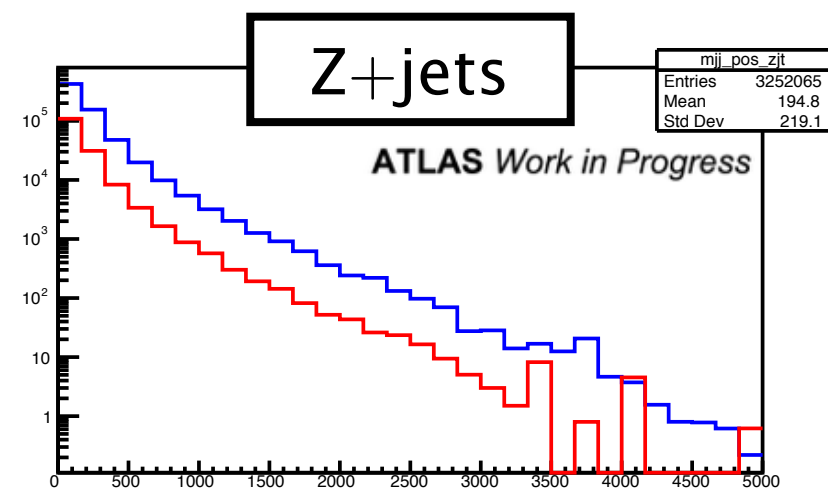
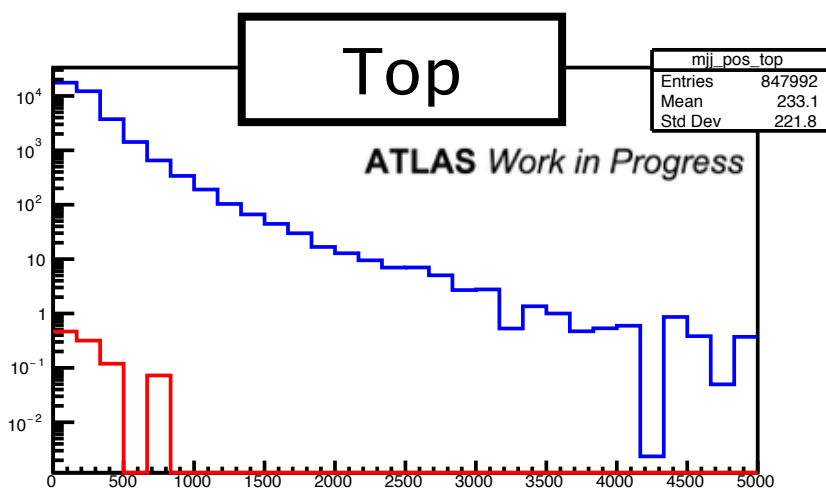
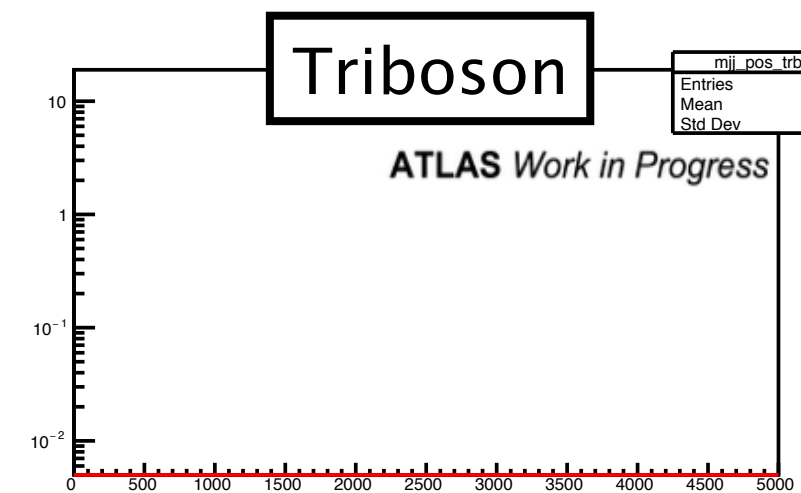
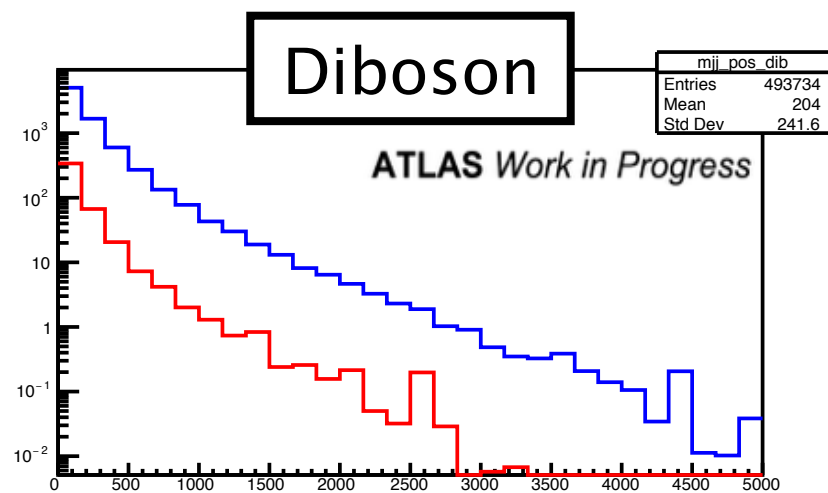
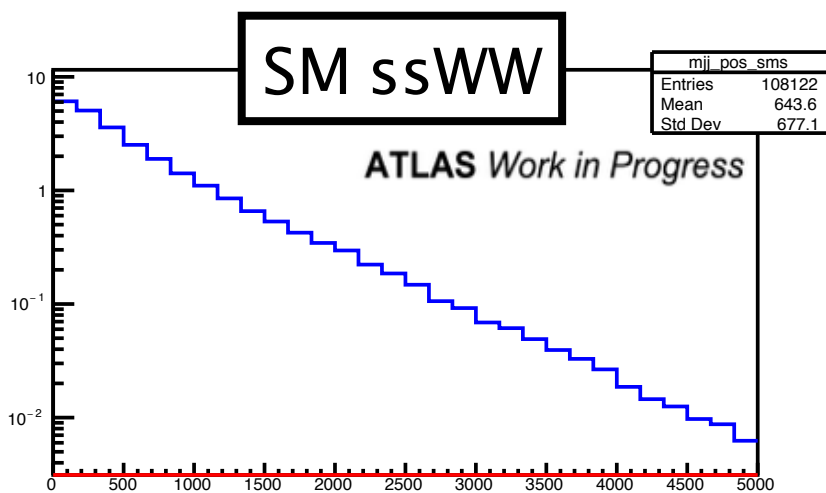
Some of our backgrounds are calculated up to NLO (diboson, top, Z+jets and W+jets). This introduces negative weights as a way to treat diagrams that would cancel out during the amplitude calculation.

TMVA does not usually consider negative weights. Built-in options to do so are experimental.

If the shape of the events with negative weights is the same as those with positive weights, the absolute value can simply be scaled down.

Channel	Diboson	Top	Z+jets	W+jets
ee	0.89	1	0.62	0.81
eμ	0.91	1	0.78	0.87
μe	0.89	1	0.75	0.54
μμ	0.90	1	0.62	0.89

Negative weights (m_{jj})



Negative Positive

Charge-flip killer (CFK)

To further refine the selection, the analysis will benefit from an ATLAS-wide tool developed at Université de Montréal, the Electron Charge ID Selector tool (commonly: charge-flip killer).

The tool uses a BDT approach to identify charge-flipped electrons based on a large amount of variables.

Current efficiency at 97% acceptance is over 90% charge-flip rejection.

The CFK is already in use by some analyses and is planned for use by many more.